Reconstruction of late 19th century geometry of Kotárjökull and Breiðamerkurjökull in SE-Iceland and comparison with the present

Snævarr Guðmundsson

Faculty of Earth Sciences
University of Iceland
2014

Reconstruction of late 19th century geometry of Kotárjökull and Breiðamerkurjökull in SE-Iceland and comparison with the present

Snævarr Guðmundsson

60 ECTS thesis submitted in partial fulfillment of a
Magister Scientiarum degree in Geology

Advisor
Helgi Björnsson

Examiner
Tómas Jóhannesson

Faculty member of MS committee: Jón Eiríksson

Faculty of Earth Sciences
School of Engineering and Natural Sciences
University of Iceland
Reykjavík, May 2014

Reconstruction of late 19th century geometry of Kotárjökull and Breiðamerkurjökull in SE-Iceland and comparison with the present

60 ECTS thesis submitted in partial fulfillment of a *Magister Scientiarum* degree in Geology

Faculty of Earth Sciences
School of Engineering and Natural Sciences
University of Iceland Sæmundargata 2
101 Reykjavík

Telephone: 525 4600

Bibliographic information:
Snævarr Guðmundsson, 2014, *Reconstruction of late 19th century geometry of Kotárjökull and Breiðamerkurjökull in SE-Iceland and comparison with the present*, M.Sc. thesis, Faculty of Earth Sciences, University of Iceland.

Printing: bbprentun
Höfn í Hornafirði, Iceland, May 2014

Abstract

Glaciers in Iceland have retreated notably since the end of the 19th century in response to climate warming. Prior to that glaciers advanced during the Little Ice Age (LIA), which lasted several centuries. The recession has had many geomorphological and hydrological effects, for example a widespread exposure of moraines and other glacial landforms, changes in river courses and crustal uplift. This thesis contributes to studies of the glacier changes with two papers. They focus on methods to construct digital elevation models (DEMs) of the outlet glaciers Kotárjökull and Breiðamerkurjökull in Öræfajökull and Vatnajökull, SE-Iceland, at the end of the LIA ~1890 as well as Breiðamerkurjökull in 1945. The DEMs are derived from several data sources including topographic maps, aerial photographs, oblique photography, remote sensing, field tracing of geomorphological features and a LiDAR DEM from 2010. Comparison of the derived ice surface elevation in ~1890 and 1945 with the 2010 DEM provides a quantitative estimate of past glacier changes since the LIA maximum. The high precision LiDAR DEM enables the correction of the topographical maps from 1904 and 1945 and the extraction of ground control points to interpret old photographs in terms of elevation changes until 2010. The changes in the glacier elevation are greatest at the termini, up to 180 m for Kotárjökull and >200 m for Breiðamerkurjökull, but decrease to near zero in the uppermost part of the accumulation area. Breiðamerkurjökull (10–1760 m a.s.l.) has retreated about 5 km since ~1890, exposing 114 km^2 of proglacial terrain and lost a volume of ~69 km^3 water equivalent (w.e.); corresponding to an average specific annual mass loss of 0.64 m w.e./yr. Kotárjökull (350–1800 m a.s.l.) retreated 1.3–2 km in the same time period, lost 2.7 km^2 of its ~1890 area and and 0.4 km^3 w.e. or 30% of its volume, corresponding to a specific mass loss rate of 0.23 m w.e./yr. The results are an encouragement to continue with estimation of other glaciers and ice caps at the end of the LIA maximum on the basis of old maps and geomorphological evidence using high-resolution, accurate maps of the present glaciers for reference.

Útdráttur

Frá lokum 19. aldar hafa miklar breytingar orðið á íslenskum jöklum. Þeir hafa hörfað og rýrnað vegna hlýnandi loftslags. Jöklarnir náðu mestu stærð á sögulegum tíma um 1890, eftir nokkurra alda kuldaskeið sem nefnt er litla ísöld. Hop þeirra hefur haft ýmis áhrif, t.d. á landmótun, farvegi vatnsfalla og landris. Þessi ritgerð samanstendur af tveim greinum um jöklabreytingar. Í þeim er greint frá aðferðum til þess að draga upp hæðarlíkön (DEM) af yfirborði Kotárjökuls í Öræfajökli og Breiðamerkurjökuls í Vatnajökli um 1890 og Breiðamerkurjökuls árið 1945. Líkönin byggja á fjarkönnunargögnum, loftmyndum, gömlum kortum, ljósmyndum, jarðfræðilegum ummerkjum á vettvangi og leysimælingu (LiDAR) jöklanna frá 2010. Með samanburði landlíkananna frá 1890 og 1945 við leysimælinguna frá 2010 fæst mat á breytingum sem orðið hafa á jöklunum síðan í lok 19. aldar. Nákvæm leysimælingin frá 2010 gerir kleift að leiðrétta skekkjur í eldri landakortum og meta hæðarbreytingar á yfirborði jökulsins út frá gömlum ljósmyndum. Breytingar í hæð jöklanna eru mestar við sporðana, allt að 180 m fyrir Kotárjökul og >200 m fyrir Breiðamerkurjökul, en litlar sem engar efst á safnsvæðum. Frá ~1890 til 2010 hopaði sporður Breiðamerkurjökuls rúma 5 km að meðaltali og um 114 km^2 lands kom undan jökli. Jafnframt rýrnaði jökullinn um 69 km^3 að vatnsgildi eða um 20%. Kotarjökull hopaði 1,3–2 km og rýrnaði um 2,7 km^2 að flatarmáli á sama tíma og rúmmál hans minnkaði um 0,4 km^3 að vatnsgildi eða um 30%. Að meðaltali missti Kotárjökull 0,23 m vatns/ár jafndreift yfir hann allan en Breiðamerkurjökull 0,64 m vatns/ár. Niðurstöður verkefnisins eru hvatning til þess að halda áfram og meta stærð annarra jökla í lok litlu ísaldar á grundvelli gamalla korta og jarðfræðilegra ummerkja með hliðsjón af nýjum, nákvæmum jöklamælingum.

Introduction

Volume and area changes of ice caps and outlet glaciers in Iceland, since the end of the 19th century, display clear impacts of climate change. The glaciers advanced during a cold period lasting several centuries, known as the Little Ice Age (LIA) (e. g. Ogilvie & Jónsson, 2000; Þórarinsson, 1943). In general the end of the LIA in Iceland is appointed to the year 1890 when many of Iceland's outlet glaciers reached their maximum late-Holocene extent. The rate of recession since then has been related to climate fluctuations (Jóhannesson & Sigurðsson, 1998). The pace of the recession has fluctuated through the period but rising strikingly after the mid 1990s (Björnsson et al., 2013). Glacier variations in Iceland have been linked to global warming and global sea level rise (e.g. Björnsson et al., 2013; Aðalgeirsdóttir et al., 2011; Axford et al., 2009; Jóhannesson et al., 2007; Magnússon et al., 2005).

The recession of glaciers in Iceland has many hydrological and geomorphological implications. The largest ice caps serve as water reservoirs for production of hydroelectricity (e. g. Björnsson and Pálsson, 2008; Jóhannesson et al., 2007). Changes of riverbeds, a side effect of retreating glaciers, has already impacted the road transportation system. A few bridges now cross empty riverbeds in Southeast Iceland, including the largest bridge in Iceland. Continued retreat of Skeiðarárjökull outlet glacier has caused Skeiðará glacial river to merge with Gígjukvísl, another glacial river of Skeiðarárjökull (e. g. Björnsson, 2009).

Crustal deformation, uplift and crustal strain release is a another impact. Glacio-Isostatic Adjustment (GIA) due to the thinning of the major ice caps in Iceland, with uplift rates up to 25 mm/year has been observed (Auriac et al., 2013; Sigmundsson et al., 2013; Árnadóttir et al., 2009; Pagli & Sigmundsson, 2008; Pagli et al., 2008). Over the last 120 years glacial recession and hence reduced ice load has modified the stress field in the Earth's crust. The deformation process provides useful information to understand the mantle rheology and crustal structure under Iceland. The reduced ice load pressure may also affect volcanic systems. Stress changes can have various consequences in magmatic systems such as modifing melting conditions, influencing magma propagation and emplacement of dykes, and magma storage zones.

Quantitative information about the loss in area and volume of glaciers since their LIA maximum extent (LIA_{max}) is important for the above mentioned hydrological and geological studies as well as for studies of the response of glaciers to climate variations. The present work is a contribution to this theme. In general the aim of the project is to constrain changes of two outlet glaciers of Vatnajökull ice cap, since the end of the 19th century to present time. This is done by a) compiling and reevaluating all available data from earlier geodetic surveys and topographic maps, aerial and oblique photographs and written historical documents, b) mapping the outline of the maximum extent of the glaciers at the end of the 19th century, as traced from field inspection of visible glacial geomorphological features (like moraines), c) produce digital elevation models of the glacier surface at various times, d) calculation of ice volume changes by differencing digital elevation models.

This thesis contains one peer reviewed paper and one paper to be submitted to a peer reviewed journal. The first, *Post-Little Ice Age volume loss of Kotárjökull glacier, SE-Iceland, derived from historical photography*, was published by Jökull in 2012. The paper is re-published here with minor spelling corrections. Co-authors of the paper are Hrafnhildur Hannesdóttir and Helgi Björnsson, who is the supervisor of this work. Kotárjökull is one of the outlet glaciers of the Öræfajökull ice cap. The evolution of this outlet since 1890's has provided valuable information about the surface elevation changes in general on Öræfajökull and Vatnajökull ice caps since the LIA_{max}. Second, *Changes of the Breiðamerkurjökull outlet glacier, SE-Iceland, from its maximum extent in the late 19th century to the present*, is planned to be submitted for publishing in 2014. This glacier is one of the largest outlet glaciers of Vatnajökull ice cap. On average, Breiðamerkurjökull has retreated more than 5 km inland since its LIA_{max} in the late 19th century when a narrow gap of few hundred meters separated the terminus from the sea (Björnsson, 2009, 1996; Watts, 1962; Thoroddsen, 1931). Two centuries earlier the nearby outlets of Öræfajökull ice cap, Hrútárjökull and Fjallsjökull, had merged with Breiðamerkurjökull, forming a continuous ice terminus with an overall width of 28.5 km.

Together with the PhD project of Hrafnhildur Hannesdóttir these projects cover the southeast region of Vatnajökull ice cap.

Contents

List of Figures

List of Tables

Abbreviations

AAR: Accumulation Area Ratio.

AMS: Army Map Series.

DEM: Digital Elevation Model.

DGS: Danish General Staff.

ELA: Equilibrium Line Altitude.

GIS: Geographic Information System.

ISN 93: Geodetic Reference System for Iceland (see web of the National Land Survey of Iceland: www.lmi.is).

LIA: Little Ice Age.

LIA_{max}: Little Ice Age maximum extent (ca. 1890).

LiDAR: (Light detection and ranging) Remote sensing technology using laser pulses to measure surface topography.

MODIS: Moderate Resolution Imaging Spectroradiometer (satellite instrument).

SPOT: Satellite Pour l'Observation de la Terre (satellite).

w.e.: water equivalent.

Acknowledgements

Compiling this thesis I have received support by individuals, institutions and funds. First of all I would like to thank my supervisor Helgi Björnsson for excellent guidance, patience and help through the project. My knowledge of glaciers has also benefited greatly from other members of the *Jöklahópur* (the glaciology group) of the Institute of Earth Sciences, University of Iceland. Especially, Finnur Pálsson guided me patiently through various scientific and technical problems. Hrafnhildur Hannesdóttir, PhD student in glaciology, collaborated with me in the study of Kotárjökull, provided field assistance in Esjufjöll/Máfabyggðir in 2012 and helped solving problems with the Surfer software. Eyjólfur Magnússon assisted regarding ice thickness, ice flow, and the response of glaciers to climate change and I had fruitful discussions with many other colleagues in Askja.

I also want to thank my good friends Einar Steingrímsson who assisted me during field work around Breiðamerkurjökull glacier outlet in 2011 and Torfi Hjaltason and Björn Vilhjálmsson. Þorsteinn Sæmundsson, PhD astronomer, and Magnús Tumi Guðmundsson for helpful discussion on calculating glacier surface elevation changes by comparing duplicate photographs. I would like to thank Tómas Jóhannesson and Jón Eiríksson for helpful comments and criticism that improved the thesis.

This study has relied heavily on the recent LiDAR maps of the glaciers in Iceland that were funded by the Icelandic Research Fund, the Landsvirkjun (the National Power Company of Iceland) Research Fund, the Icelandic Road Administration, the Reykjavík Energy Environmental and Energy Research Fund, the Klima- og Luftgruppen (KoL) reseach fund of the Nordic Council of Ministers, the Vatnajökull National Park, the organisation Friends of Vatnajökull, the National Land Survey of Iceland and the Icelandic Meteorological Office.

This project has been supported financially by following institutions and research funds:

Náttúrustofa Suðausturlands, The South East Iceland Nature Center.

SVALI, Nordic Centre of Excellence SVALI, Stability and Variations of Arctic Land Ice, funded by the Nordic Top-level Research Initiative (TRI).

Kvískerjasjóður provided grants for the research projects.

Landsvirkjun, the National Power Company of Iceland provided student grants.

Jöklarannsóknafélag Íslands, Glaciological Society of Iceland provided technical support for field studies.

1 Post-Little Ice Age volume loss of Kotárjökull glacier,SE-Iceland, derived from historical photography

Snævarr Guðmundsson, Hrafnhildur Hannesdóttir and Helgi Björnsson
Institute of Earth Sciences, University of Iceland, Sturlugata 7, 101 Reykjavík, Iceland
Corresponding author: snaevarr@mmedia.is

Abstract *– Kotárjökull is one of several outlet glaciers draining the ice-covered central volcano Öræfajökull in SE-Iceland. We estimate the average annual specific mass loss of the glacier, to be 0.23 m (water equivalent) over the post Little Ice Age period 1891–2011. The glacial retreat accounts for an area decrease of 2.7 km^2 (20%) and a volume loss of 0.4 km^3 (30%). A surface lowering of 180 m is observed near the snout decreasing to negligible amounts above 1700 m elevation. This minimal surface lowering at high altitudes is supported by a comparison of the elevation of trigonometrical points on Öræfajökull's plateau from the Danish General Staff map of 1904 and a recent LiDAR-based digital elevation model. Our estimates are derived from a) three pairs of photographs from 1891 and 2011, b) geomorphological field evidence delineating the maximum glacier extent at the end of the Little Ice Age, and c) the high-resolution digital elevation model from 2010–2011. The historical photographs of Frederick W.W. Howell from 1891 were taken at the end of the Little Ice Age in Iceland, thus documenting the maximum glacier extent.*

1.1 Introduction

The first descriptions of the Little Ice Age (LIA) glacier margins in Iceland were collected in the proximity of inhabitated regions south of Vatnajökull ice cap. Occasional reports descend from travellers passing through rural districts in the 18th and 19th centuries (e.g. Þórarinsson, 1943; Björnsson, 2009). Less attention was paid to the smaller outlet glaciers, although sparse observations were made during traverses on the glaciers. A number of photographs of Icelandic glaciers from the late 19th and early 20th century are preserved (Ponzi, 2004; Archives of the National Land Survey of Iceland; Reykjavík Museum of Photography; National Museum of Iceland). They provide valuable information on glacier extent, and can be analyzed by repeat photography to deduce glacier changes. This approach has been used world-wide, and was first practiced to document glacier variations in the European Alps in the late 1880s (see e.g. Harrison, 1960; Luckman et al., 1999; Molnia, 2010; Webb et al., 2010; Fagre, 2011).

In this paper we present unique historical oblique photographs of Kotárjökull outlet glacier (Figures 1 and 2) from the first ascent of Hvannadalshnúkur (the highest peak in Iceland) in Öræfajökull in 1891 (Guðmundsson, 1999). They were taken by an English traveller, Frederick W. W. Howell (1857–1901), who together with two companions from the farm Svínafell (Páll Jónsson and Þorlákur Þorláksson) reached the summit on 17th of August. The photographs are among the first prints of glaciers in Iceland, and were taken at the 1890 LIA maximum stage (e.g. Þórarinsson, 1943). His photographs are used to derive the geometry of the LIA maximum glacier, by trigonometric calculations, and by including information from present-day photographs, geomorphological evidence and a detailed digital elevation model

(DEM). Our findings allow quantitative estimates of glacier mass change over the last 120 years. We also compare the 1904 map of the Danish General Staff (Herforingjaráðið, 1905) of Öræfajökull's plateau, at an altitudinal range of 1700–2100 m, with a recent DEM, to get an estimate of glacier surface changes there during this time period.

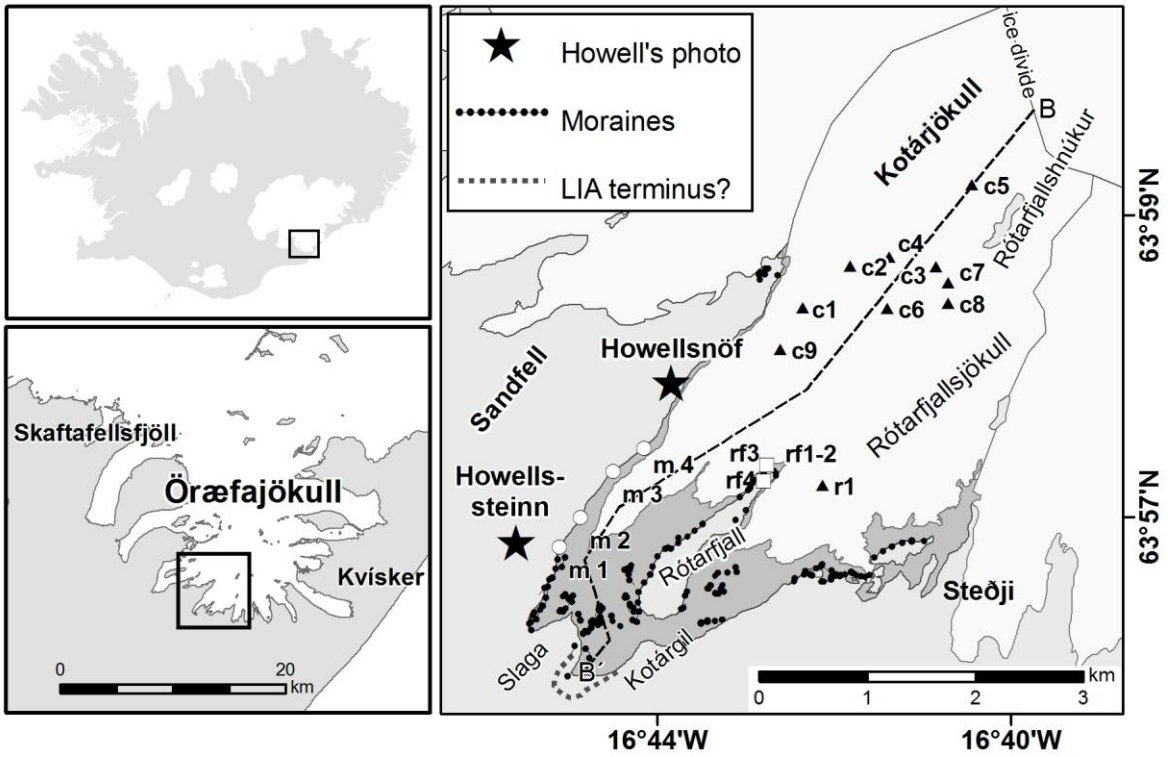

Figure 1. Kotárjökull glacier flows southwest from Öræfajökull ice cap. The eastern branch of the glacier is named Rótarfjallsjökull. The white area delineates the glacier's extent in 2011, whereas the middle-gray area indicates the glacier outline at the LIA maximum. The ice divide inside the rim of the Öræfajökull caldera, lies at approximately 1800 m. Crevasse areas (black triangles) are used to calculate glacier surface changes between 1891 and 2011. Black dots represent lateral moraines used to reconstruct the maximum glacial extent in the gorge, and white circles and boxes indicate sites where surface changes are estimated from geomorphological and photographic evidence. Line B-B' is a longitudinal profile for later discussion.

1.2 Research area

Öræfajökull is a 2000 m high ice-capped central volcano. The ice-filled caldera is 5 km wide and 500 m deep, with an ice volume of 4.6 km^3 (Björnsson, 1988; Magnússon et al., 2012). Ice flows over the caldera rim and forms several outlet glaciers. The ice thickness of Kotárjökull is on average 100 m, approximated from the surface slope of the glacier (Magnússon et al., 2012). The glacier plateau receives the highest amounts of annual precipitation in Iceland, 5700–7800 mm w.e., almost entirely falling as snow (Björnsson et al., 1998; Guðmundsson, 2000). Comparison with observed precipitation from the nearest lowland meteorological station Kvísker (Figure 1), implies that the precipitation on the ice cap is twice as high as on the lowlands to the southeast of Öræfajökull (Guðmundsson, 2000).

Kotárjökull covers at present about 11.5 km^2, with an average slope of 20°, and the equilibrium line lies around 1100–1200 m. Heading from an elevation of 1800 m, inside the caldera, the glacier is split into two branches by Rótarfjall mountain (946 m): the main branch terminating in a 300–400 m wide gorge (Figures 1 and 2). The eastern branch goes by the

name Rótarfjallsjökull. These glaciers surrounded Rótarfjall, and merged together in Kotárgil at the end of the 19th century (Thoroddsen, 1896). Parts of the terminal moraine northwest and east of Slaga mountain are obscure and may be remnants of an older stage. No dead ice is observed in the glacier's marginal area.

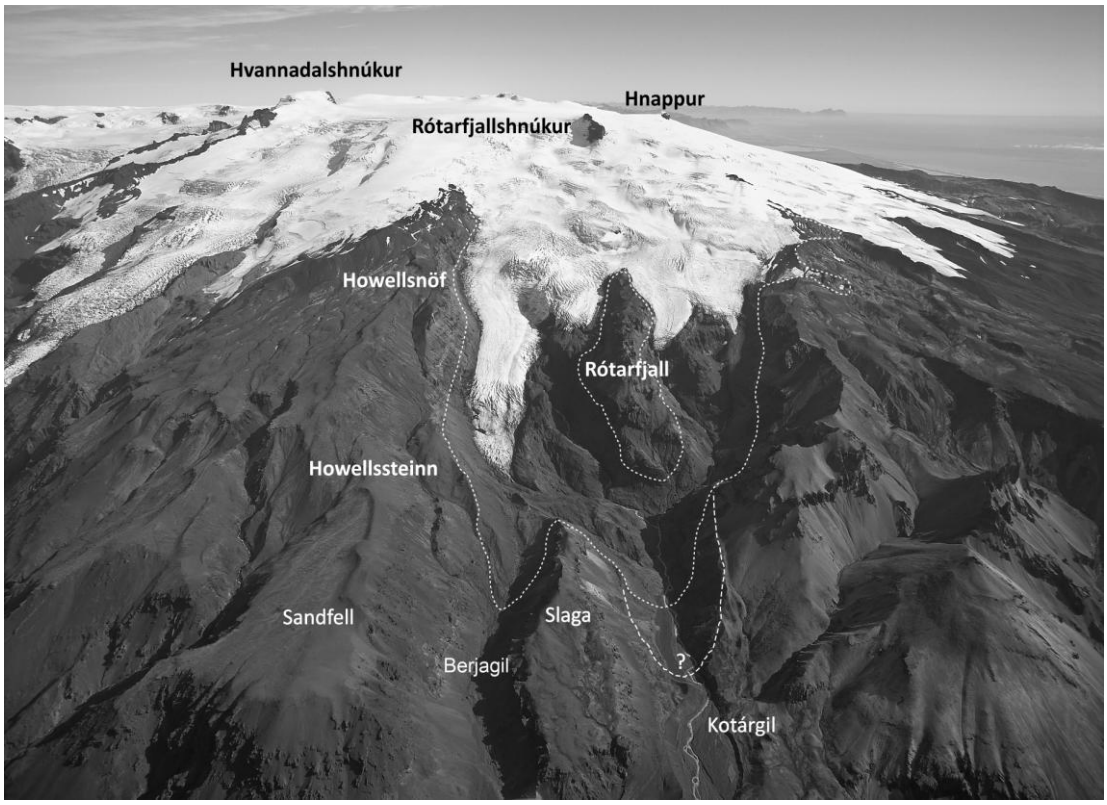

Figure 2. Oblique arieal photograph of Öræfajökull and Kotárjökull. The maximum LIA glacier extent is marked with a dotted line. Traces of the terminus in Kotárgil are obscure, especially east of Slaga, hence two possible margin positions are presented. Photo: Snævarr Guðmundsson [hereafter SG] 17 August 2006.

1.3 Data

Howell's photographs were taken from two locations on Sandfell mountain (Figures 1 and 2): a) one shot towards east to Rótarfjall from Howellssteinn (N63.9497°, W16.7587°, elevation 573 m a.s.l.) and b) two shots from Howellsnöf (N63.9624°, W16.7286°, elevation 1020 m), 1) northeast towards Rótarfjallshnúkur (1833 m) across the upper reaches of the glacier, and 2) east towards Rótarfjall. Howellssteinn and Howellsnöf are not geographical place names, but used as landmarks by the authors. The photographs confirm that the highest lateral moraines, trimlines and glacial erratics in the narrow gorges of Kotárgil and Berjagil (Figure 2) are from the 1890 LIA maximum. In November 2011 the two locations were revisited, the photos reframed and the acquired duplicates (Figures 3a-b, 4a-b and 5a-b) used to calculate the recession of the glacier between 1891 and 2011. Howell's photographs are available in the Fiske Icelandic Collection, at the Cornell University Library website.

High-resolution aerial images of Loftmyndir ehf© (2003) were used to outline the LIA maximum glacier. In situ and oblique aerial photographs of 2006 and 2010, helped derive the glacial extent.

A recent DEM, produced from airborne LiDAR measurements in August 2010 and September 2011 (data from the Icelandic Meteorological Office and the Institute of Earth Sciences, University of Iceland, 2011; Jóhannesson et al., 2013), provides accurate positions and elevations (Table 1). The DEM has horizontal resolution of 5x5 m and vertical accuracy within 0.5 m. It provides precise elevation of the lateral moraines and trimlines.

1.4 Methods

The extent of Kotárjökull at the LIA maximum, was based on photographic and geomorphological evidence, and the LiDAR DEM providing basic topographical data. The glacier margin in the ablation area, is delineated from the highest lateral moraines, glacial erratics, and trimlines. Data on elevation changes above the equilibrium line are restricted to the old photographs. The idea of obtaining quantitative estimates of glacier changes from the photographic duplicates, originates from methods used in astrometry. The movements of distant objects are measured over time from separate images, taken hours to decades apart.

1.4.1 Repeat photography

The three photographic pairs of Kotárjökull were collimated in GIS ArcMap (Figures 3a-b, 4a-b, 5a-b). A 3D-image, a duplication of Figure 3b, was produced from the DEM in ArcScene, to improve the accuracy of our measurements. The southeastern flank of Rótarfjallshnúkur has apparently undergone some landform changes since 1891, perhaps a landslide. The photos in Figures 3a-b were collimated, using the northern (I) and southern (II) peaks of Rótarfjallshnúkur for reference, the top of Sandfell (III), and a crevasse area (IV) on the horizon to the west of Rótarfjallshnúkur (Figure 6). The photographs in Figures 4a-b were referenced with four points, and in Figures 5a-b, with 10 points. The ease of collimating the duplicate photos, indicates minimal errors related to the older camera's lens distortion.

Nine crevasse areas in the accumulation area (Figures 3a-b), were used for surface elevation calculations. The lowering was measured in pixel units and converted to metres. A total of 7 measurements evenly distributed over each crevasse bulge, from center towards left (l_{1-3}) and right (r_{1-3}), were used to obtain a mean pixel value for the surface lowering (Figure 6 and Table 1). Two independent routines to calculate the glacier surface changes in metres were used.

1.4.2 Routine 1

The vertical glacier surface change (Δh) at any distance (d) from the site of photography was estimated by scaling in metres the pixel unit size ($\theta_u = H/n_m$) based on a known vertical height of a mountain cliff (H spanning n_m pixels) at a known distance (D_o), in this case Rótarfjallshnúkur (Figure 6). If the measured surface lowering of a crevasse area in pixel units is n_c, the corresponding glacier surface change in metres is:

$$\Delta h = \theta_u \times (d/D_o) \times n_c$$

The northern face of Rótarfjallshnúkur is 60 m high (H_I) and n_{mI} = 30 pixels, hence θ_{uI} = 2.0 m/pixel; the distance to the face from Howellsnöf is D_I = 3.650 m (Figure 6). The southern face is H_{II} = 120 m and n_{mII} = 52 pixels, hence θ_{uII} = 2.3 m/pixel and the distance from Howellsnöf D_{II} = 3.320 m.

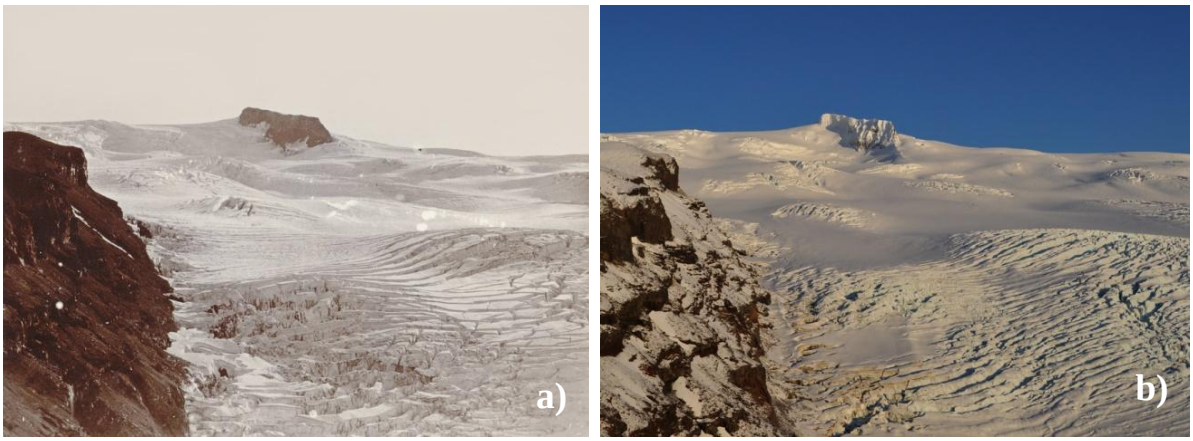

Figure 3. The photographic pair of Kotárjökull and Rótarfjallshnúkur, view from Howellsnöf on Sandfell. – a) Kotárjökull og Rótarfjallshnúkur, útsýni frá Howellsnöf. Photos./Myndir. Howell 17 August 1891 (a) and SG 3 November 2011 (b).

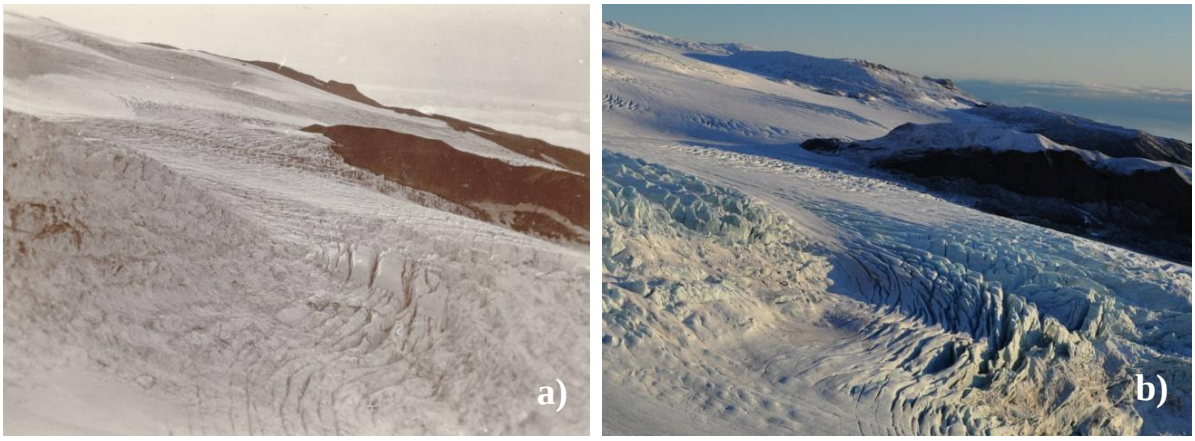

Figure 4. Kotárjökull (near) and Rótarfjallsjökull divided by Rótarfjall, view from Howellsnöf on Sandfell. Steðji outcrop in the background.. Photos./Myndir. Howell 17 August 1891 (a) and SG 3 November 2011 (b).

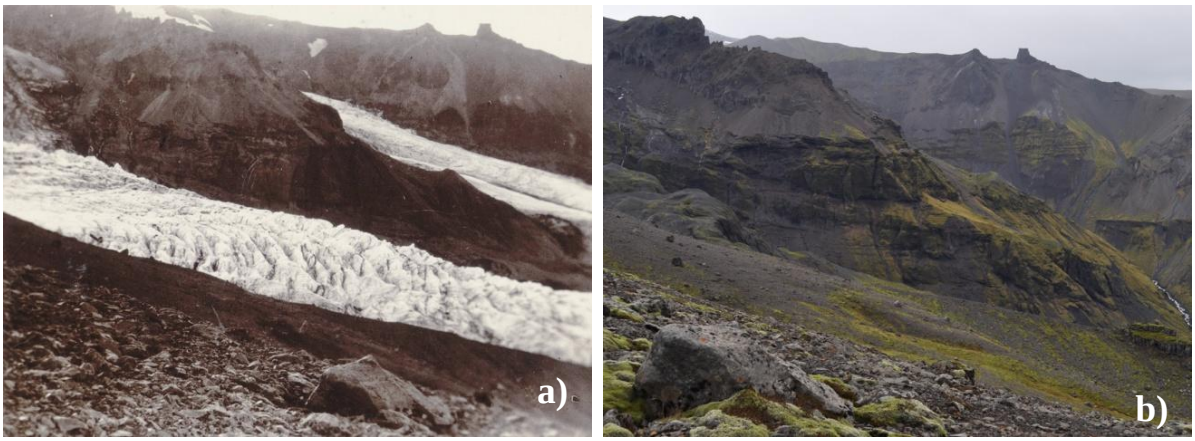

Figure 5. Kotárjökull and Rótarfjallsjökull, view from Howellssteinn. In August 1891 the glaciers merged together in front of Rótarfjall, flowing into Kotárgil. Photos./Myndir. Howell 17 August 1891 (a) and SG 3 November 2011 (b).

To test the quality of θ_u as a satisfactorily accurate value, we calculated the size of θ_{uII} at distance D_I ;

$$(\theta_{uII} \times D_I)/ D_{II} = \theta_{uII} / D_I = 2.5 \text{ m/pixel}$$

and then obtained an average value for θ_{uI} of 2.25 m/pixel (θ_u) at distance D_I, which was used for all calculations. Glacier surface changes were also calculated for crevasse area r_1 (Figures 1 and 4a-b), using routine 1.

Table 1. Dimensions of the crevasse areas, and surface elevation change measurements in pixel units. – Tafla 1. Grunnupplýsingar um sprungukollana (c1–c9) sem notaðar voru til þess að reikna yfirborðslækkun. Meðalhæðarbreyting (í myndeiningum) út frá 7 mælingum á hverjum sprungukolli.

						measurements (pixels)							
area	**latitude**	**longitude**	**altit. (m)**	**d (m)**	**bearing°**	**l_1**	**l_2**	**l_3**	**center**	**r_1**	**r_2**	**r_3**	**Δθ**
c1	63.9683	16.7031	1166	1405	60.2	14.36	14.92	13.40	13.2	13.25	12.83	10.02	13.14
c2	63.9716	16.6939	1319	1977	56.7	5.73	5.73	6.33	5.29	4.62	4.73	3.85	5.18
c3	63.9722	16.6865	1398	2328	59.9	5.76	5.19	4.05	5.76	5.99	5.85	5.99	5.51
c4	63.9713	16.6778	1429	2673	66.2	2.86	2.36	2.29	2.86	2.86	2.86	2.92	2.72
c5	63.9779	16.6703	1677	3335	56.60	2.36	2.29	2.36	1.81	1.81	1.81	1.81	2.04
c6	63.9680	16.6872	1283	2113	70.80	4.62	4.01	3.49	5.29	5.19	6.41	8.05	5.29
c7	63.9697	16.6790	1367	2723	70.00	1.72	1.72	1.72	1.72	1.72	2.29	1.72	1.80
c8	63.9682	16.6757	1403	2666	73.90	2.92	3.63	3.49	2.92	2.92	3.49	2.06	3.06
c9	63.9650	16.7077	1083	1058	72.50	13.78	13.88	11.70	15.5	15.59	16.60	16.07	14.73

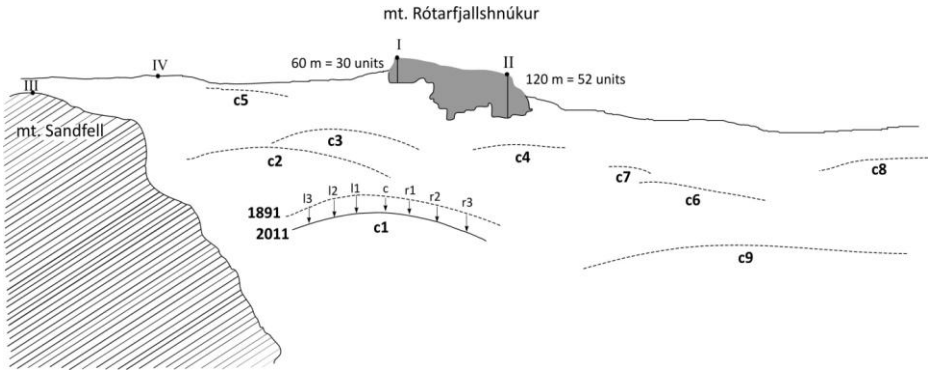

Figure 6. A sketch of the crevassed accumulation area of Kotárjökull. The edge of each crevasse area in 1891 (c1-c9) shown as a dotted line. Surface lowering of each area derived from 7 points, as illustrated for crevasse area c1. Collimation points for the two photos are indicated in Roman numerals (I-IV).

Table 2. Surface elevation changes measured by routine 1.

area	**Δθ (px)**	**θ_u (m/px)**	**Δh (m)**
c1	13.14	0.91	11.4
c2	5.18	1.28	6.3
c3	5.51	1.50	7.9
c4	2.72	1.73	4.5
c5	2.04	2.15	4.2
c6	5.29	1.36	6.9
c7	1.80	1.76	3.0
c8	3.06	1.72	5.0
c9	14.73	0.68	9.6

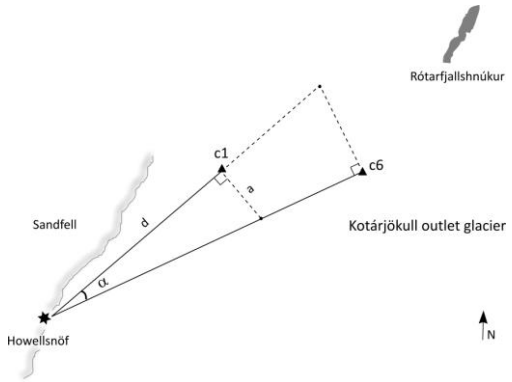

Figure 7. A scheme explaining routine 2. See text for explanation.

1.4.3 Routine 2

The pixel unit size, which is used as a reference for surface elevation changes, was determined from the photographs by calculating a lateral scaling distance ($a = d \tan \alpha$) perpendicular to the line of sight from Howellsnöf to each distinct crevasse area. The distance from the site of photography is d, and α the angle between two crevasse areas, as seen from Howellsnöf (Figure 7). The length of the opposite side is used to find the size of the pixel unit at distance d. Since the measured surface lowering in pixel units ($\Delta\theta$) is a certain ratio of the opposite side, we can calculate the change in metres at a distance d from the site of photography:

$$\Delta h = \Delta\theta \, (d \tan \alpha)/n$$

where n is the number of pixels of the corresponding angle α. This is possible since horizontal and vertical scales of the pixels are the same. We can extend the triangle's hypotenuse, depending on the point we aim at (illustrated by the dotted line in Figure 7).

Table 3. Surface elevation changes measured by routine 2. Three calculations for each crevasse area, and the lowering presented in the last column with the relevant area in parenthesis.

area	α	a (px)	Δh (m)	Δh (m)
c1→c9	12.3	394	10.2 (c1)	8.6 (c9)
c1→c8	13.7	429	10.5 (c1)	3.7 (c8)
c1→c6	10.6	329	10.5 (c1)	6.4 (c6)
c2→c6	14.1	441	5.8 (c2)	6.4 (c6)
c2→ c8	17.2	534	5.9 (c2)	4.7 (c8)
c2 →c4	9.5	293	5.8 (c2)	4.1 (c4)
c3→c2	3.2	101	7.1 (c3)	5.7 (c2)
c3→c7	10.1	312	7.3 (c3)	2.8 (c7)
c3→c4	6.3	194	7.3 (c3)	4.1 (c4)
c4→c7	3.8	118	4.1 (c4)	2.7 (c7)
c4→c6	4.6	152	3.8 (c4)	5.9 (c6)
c7→c8	3.9	125	2.7 (c7)	4.4 (c8)
c9→c3	12.6	429	8.1 (c9)	6.7 (c3)
c9→c2	15.8	519	8.5 (c9)	5.6 (c2)
c4→c5	9.6	308	4.0 (c4)	3.7 (c5)
c3→c5	3.3	120	6.2 (c3)	3.3 (c5)
c1→c5	3.6	187	6.2 (c1)	2.3 (c5)

1.4.4 The LIA glacier and volume calculations

We assume unchanged glacier geometry in the accumulation area, as seen from the photos in Figures 3a-b. Calculated elevation changes were used to raise the contour lines of the LiDAR DEM to an 1891 level. The reconstructed cross-valley profiles of the two branches, below the equilibrium line, are convex, with a maximum height of 20 m at the glacier center line. This assumption is based on the photographs in Figures 4a-b and 5a-b. Our estimate for the uncertainty limits of the reconstructed 1891 surface is ±2 m. A gradual thickness changes along the longitudinal profile of Kotárjökull is assumed (Figure 1), and interpolated between data thickness points using a least-squares fit to a log-linear equation. The volume loss of Kotárjökull was calculated by subtracting the glacier surface of 2011 from the reconstructed surface of 1891.

1.4.5 Elevation changes on the plateau of Öræfajökull

The 1904 map of Öræfajökull of the Danish General Staff was georeferenced with the LiDAR DEM, and the elevation of selected trigonometrical points from the older map compared with the DEM, to resolve possible glacier surface changes. Nine geodetic points on mountain peaks or nunataks and eleven on the glacier surface were selected for this purpose, spanning an altitudinal range of 1700–2100 m.

1.5 Results

1.5.1 Surface elevation changes

Crevasse areas were used to calculate elevation changes in the accumulation zone (Tables 1, 2 and 3). Routines 1 and 2 give similar results, showing an average difference of 1.1 m, with routine 1 always giving higher values (Table 4). Surface changes above 1700 m were negligible, and 4–11 m from there down to the equilibrium line. The lowering gradually increasing, 20–30 m north of Rótarfjall (Figures 4a-b and Table 5), and reaching a maximum of 180 m in Kotárgil (Figures 8, 9 and Table 5.

Table 4. Comparing the surface elevation changes of Kotárjökull above 1100 m elevation, calculated by the two routines.

crevasse area	Δh (routine 1)	Δh (routine 2)	difference in Δh between routines
c1 (1166 m)	11.4 m	9.4 m	2.0 m
c2 (1319 m)	6.3 m	5.8 m	0.5 m
c3 (1398 m)	7.9 m	6.9 m	1.0 m
c4 (1429 m)	4.5 m	4.0 m	0.5 m
c5 (1677 m)	4.2 m	3.1 m	0.9 m
c6 (1283 m)	6.9 m	6.2 m	0.7 m
c7 (1367 m)	3.0 m	3.1 m	0.1 m
c8 (1403 m)	5.0 m	4.3 m	0.7 m
c9 (1083 m)	9.6 m	8.4 m	1.2 m

1.5.2 Area and volume changes

Glacial retreat and the volume loss of Kotárjökull is based on the inner margin in Kotárgil. The terminus of Kotárjökull has retreated 1.3 km, since the LIA maximum, from an elevation of 175 m to 350 m (Figure 9). Rótarfjallsjökull has retreated ca. 2 km, and the terminus is currently at an elevation of 660 m. The eastern branch, with a small part of the accumulation area extending up to the ice cap plateau, has on average retreated 17 m/yr, whereas the main branch shows a mean recession of 11 m/yr. Rótarfjallsjökull receives less ice from the caldera and has a smaller accumulation area. The glacier area has decreased from 14.5 to 11.5 km^2 (20%), and the volume loss has been approximately 0.4 ±0.02 km^3, relative to the uppermost LIA_{max} glacier margin in Kotárgil (Figure 1). Given the average glacier thickness of 90 m (Magnússon et al., 2012), Kotárjökull has lost approximate 30% of its volume. Evenly spread over the mean glacier area, the recession corresponds to a loss of about 0.23 ±0.01 m w.e./yr.

*Table 5. Surface elevation change in the ablation area deduced from Figures 4a, 4b, 5a, 5b and lateral moraines and other geomorphological features in Kotárgil. *Reference landscape.*

data points	latitude	longitude	altitude 2011 (m)	altitude 1891 (m)
r1 (crevasse area)	63.9536	16.7007	950	982
rf1 (peak of Rótarfjall)	63.9547	16.7091	946	–
rf2 (N tip of Rótarfjall)	63.9540	16.7118	936	–
rf3* (W side of Rótarfj**)**	63.9554	16.7110	881	911
rf4* (W side of Rótarfj**)**	63.9544	16.7126	840	872
steðji1 (ref. landscape)	63.9420	16.6801	970	–
steðji2 (ref. landscape)	63.9412	16.6810	960	–
m4 (lateral moraine)	63.9571	16.7341	650	720
m3 (lateral moraine)	63.9553	16.7400	570	660
m2 (lateral moraine)	63.9520	16.7466	400	510
m1 (lateral moraine)	63.9492	16.7507	340	520

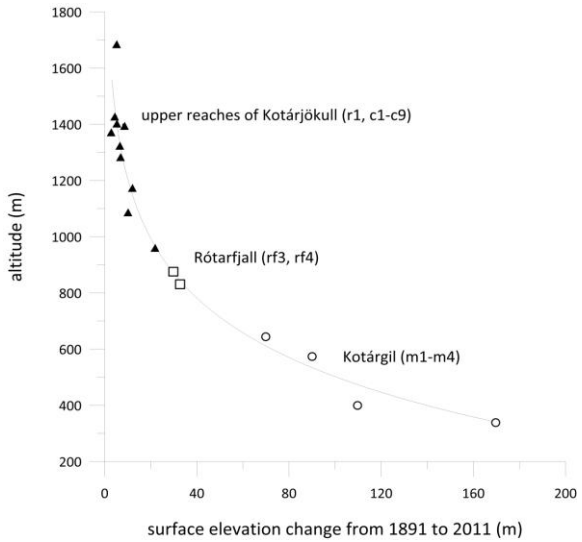

Figure 8. Surface elevation changes of Kotárjökull along profile B'B derived from photographic evidence, lateral moraines and trimlines along the edge of the glacier. Symbols in accordance to Figure 1, triangles represent the averaged thickness change by routine 1 and 2. Few lateral moraines could be used to estimate glacier thickness change in the lower parts of Kotárgil gorge due to the uneven valley floor.

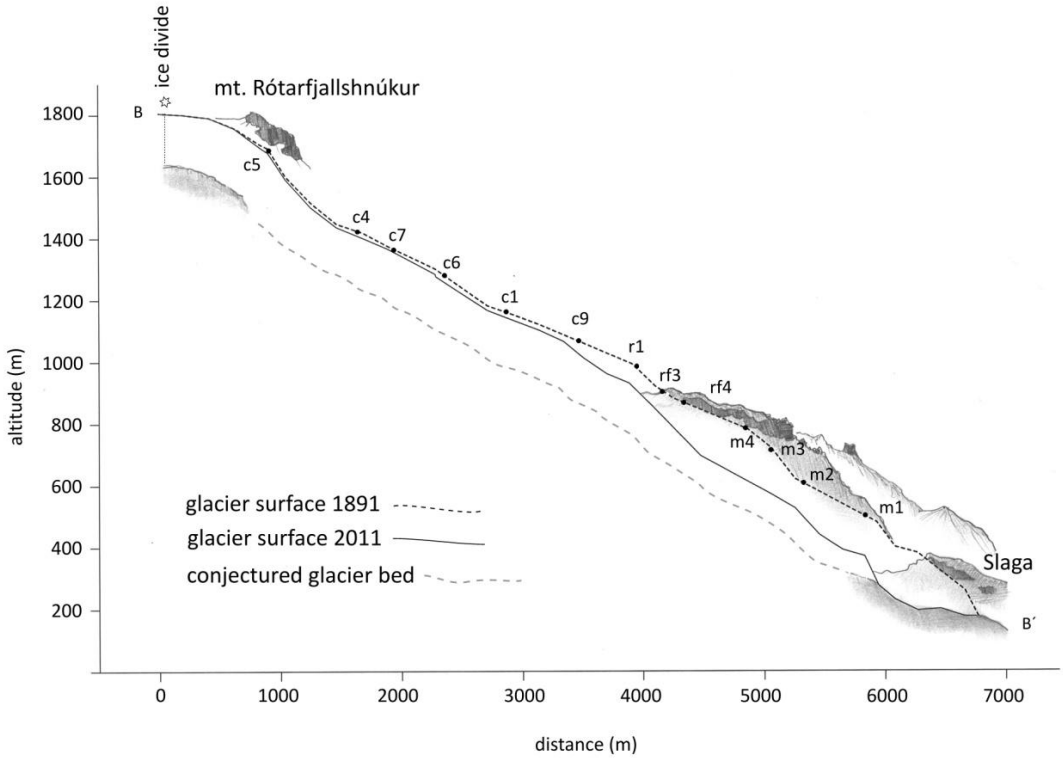

Figure 9. Profile BB' (Figure 1 for location) of Kotárjökull showing the 2011 surface, based on the LiDAR DEM, and in 1891, based on calculations of surface elevation changes of crevasse areas (c1–c9 and r1), lateral moraines in Rótarfjall (rf3 and rf4) and in Kotárgil (m1–m4). The ice thickness at the ice divide is known from radio-echo sounding measurements to be approximately 150 m. The glacier bed (dotted gray line) is sketched elsewhere, based on a correlation between ice thickness and surface slope (Magnússon et al., 2012).

1.5.3 Surface lowering on the glacier plateau

To resolve possible elevation changes of the ice plateau of Öræfajökull, the 1904 map and the 2011 DEM were compared (Figures 10a-b). Minor distortion was observed on the plateau, compared to the level of deviation in the lower rugged terrain of the mountain massif. The difference in elevation registered on the trigonometrical points above 1700 m is shown in Table 6. The elevation of the glacier points is on average 12.3 m higher on the 1904 map than the LiDAR DEM, and 11.9 m higher on the peaks or nunataks. This dissimilarity also applies to the ice-covered Hvannadalshnúkur. The peak was measured in 1904 at an altitude of 2119 m. The summit is 2110 m high according to the new DEM, which confirms recent measurements by the Glaciological Society of Iceland (1993 and 2004) and the National Land Survey of Iceland in 2005 (Guðmundsson, 2004; Morgunblaðið, 7th of August 2005). The surveying of the Öræfajökull ice cap by the Danish General Staff, was based on optical triangulation in several steps over long distances from the lowland with intermediate points on peaks in Öræfajökull and Skaftafellsfjöll (Figure 1, Koch, 1905).

*Table 6. Selected trigonometrical points on the glacier plateau (g) and peaks (p) of Öræfajökull ice cap, used to compare their elevation (see Figure 10a-b) from the LiDAR DEM and the 1904 map. Locations from the LiDAR DEM. * Difficult to locate precisely.*

Location		x (m)	y (m)	z_{LiDAR} (m)	$z_{1904\ map}$ (m)	Δz (m)
a)	Sveinstindur (p)	64.0095	16.6181	2033	2044	11
b)	Eystri Hnappar (p)	63.9799	16.6243	1753	1758	5
c)	Vestari Hnappar (p)	63.9755	16.6382	1838	1851	13
d)	Rótarfjallshnúkur (p)	63.9769	16.6613	1833	1848	15
e)	Dyrhamar (p)	64.0074	16.7014	1902	1911	9
f)	Hvannadalshryggur (p)	64.0068	16.7070	1830	1841	11
g)	west face of Hvannadalshnúkur (p)	64.0120	16.6924	1870	1879	9
h)	Tindaborg (p)	64.0240	16.6993	1727	1747	20
i)	Þuríðartindur (p)	64.0817	16.6382	1727	1741	14
j)	Hvannadalshnúkur (g)	64.0142	16.6771	2110	2119	9
k)	center of caldera (g)	64.0048	16.6392	1843	1845	2
l)	ice divide of Hrútárjökull[1] (g)	64.0012	16.6098	1912	1927	15
m)	ice divide of Hrútárjökull[2] (g)	63.9982	16.5932	1827	1840	13
n)	Tjaldskarð (g)	64.0421	16.6617	1824	1844	20
o)	Snæbreið (g)	64.0256	16.6457	2028	2041	13
p)	Jökulbak (g)	64.0531	16.6752	1911	1922	11
q)	peak NE of Sveinstindur (g)	64.0144	16.6102	1951	1962	11
r)	SW rim of caldera (g)	63.9904	16.6801	1815	1846	31
s)	acc. area of Fjallsjökull[1] (g) *	64.0576	16.6451	1710	1716	6
t)	acc. area of Fjallsjökull[2](g) *	64.0496	16.6550	1807	1808	1

1.6 Discussion

Surface elevation changes of Kotárjökull are negligible at high elevations, increasing to maximum thinning of 180 m, of the former terminus in the gorge. Nowhere else along the southeastern edge of Vatnajökull, are glacier surface elevation changes since the LIA maximum recorded continuously downward from the ice divide to the terminus. The surface lowering at the glacier snout is similar to what has been observed on other outlet glaciers of Vatnajökull to the west and east of Kotárjökull (Hannesdóttir et al., 2012). Comparable total volume loss over the 20th century is reported for Hoffellsjökull and its neighbouring southeastern outlet glaciers, on the order of 20–30% (Aðalgeirsdóttir et al., 2011; Hannesdóttir et al., 2012). The well-preserved lateral moraines are only found below the equilibrium line, hence little field evidence attests to the former high stands of the glacier in the accumulation area at its maximum extent during the LIA. The historical oblique photographs and the 1904 survey of the Danish General Staff are the only source of information for surface changes in the accumulation area.

No elevation change of the 5 km wide glacier plateau covering the caldera is remarkable. The ice cap has limited possibilities to expand, since any surplus in mass balance will flow straight over the caldera rim to lower elevations. The observed thickness change with altitude between

the end of the 19th century and 2011 on Kotárjökull, provides a reference for further studies of other outlet glaciers of Öræfajökull and the southern edge of Vatnajökull.

The observed elevation anomaly of the trigonometrical points, along with calculated surface changes in the accumulation area, raises the question whether the geodetic survey of the plateau of Öræfajökull may have been inaccurate by about 10 m (see Table 6). We speculate whether this is due to errors, i.e. caused by light refraction, across a surface with variable reflectance and changing temperature conditions (as described in Böðvarsson, 1996). We therefore doubt, that Hvannadalshnúkur has lowered by 9 m during the last 100 years, due to glacial melting, as a simple comparison of the 1904 map and recent measurements may indicate (Morgunblaðið, 2005).

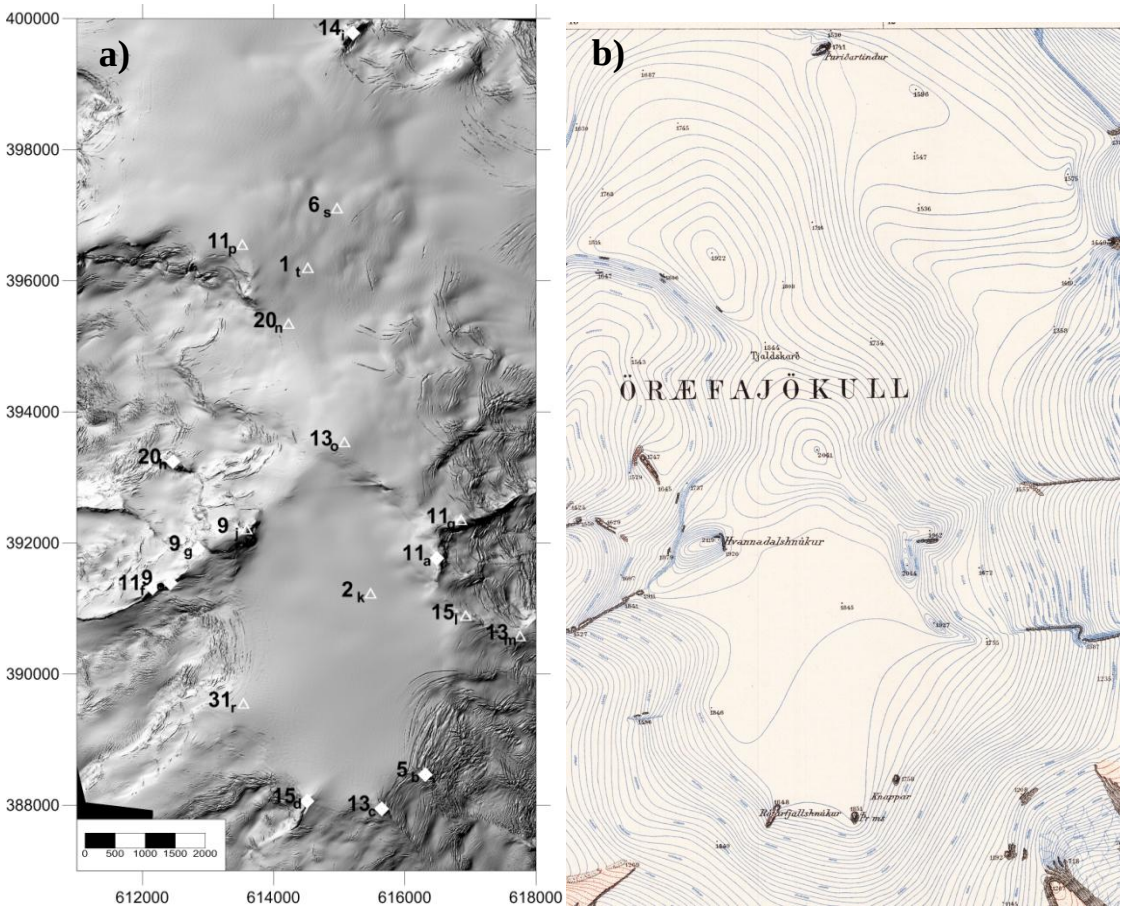

Figure 10. Elevation difference of selected trigonometrical points on the high plateau of Öræfajökull ice cap, between a) the LiDAR DEM (2010) and b) the 1904 map of the Danish General staff. Squares indicate points on the glacier, and filled circles represent points on nunataks. Each location is marked with a letter corresponding to Table 6.

1.7 Summary

By combination of several photographic archives, a recent DEM and field inspection, we delineate the area and volume loss of Kotárjökull glacier since the LIA maximum in the late 19th century. The thinning is negligable above 1700 m and gradually increases downglacier to 180 m near the terminus. The glacier has lost a volume of 0.4 km^3 (30%) and decreased in area by 2.7 km^2 (20%). We estimate an average specific mass loss of 0.23 m w.e./yr. Comparison of the Danish map from 1904 with the LiDAR DEM, indicates that little or no

elevation changes took place during the 20th century on the Öræfajökull plateau. This also applies to the summit Hvannadalshnúkur, and we suggest that lowering of Hvannadalshnúkur indicated by the 1904 DGS map may be explained by surveying errors rather than surface lowering due to reduced glacier mass balance.

Acknowledgements

With permission from the Icelandic Meteorological Office and the Institute of Earth Sciences at the University of Iceland we were able to use the LiDAR-data on a processing stage. We thank Þorsteinn Sæmundsson, astronomer, and Magnús Tumi Guðmundsson for helpful discussion on calculating glacier surface elevation changes by comparing duplicate photographs. Discussions with Eyjólfur Magnússon and Finnur Pálsson on ice thickness, ice flow, and the response of glaciers to climate change are acknowledged. The authors appreciate constructive comments by two reviewers, Patrick Appelgate and Þorsteinn Þorsteinsson. This publication is contribution number 17 of the Nordic Centre of Excellence SVALI, Stability and Variations of Arctic Land Ice, funded by the Nordic Top-level Research Initiative (TRI).

2 Changes of the Breiðamerkurjökull outlet glacier, SE-Iceland, from its maximum extent in the late 19th century to the present

Snævarr Guðmundsson[1,2], Helgi Björnsson[2], Finnur Pálsson[2], Hrafnhildur Hannesdóttir[2]
[1]*Nature Research Center of Southeast Iceland, Litlubrú 2, Höfn í Hornafirði, Iceland*
[2]*Institute of Earth Sciences, University of Iceland, Sturlugata 7, 101 Reykjavík, Iceland*
Corresponding author: snaevarr@nattsa.is

Abstract *– We have reconstructed digital elevation models (DEMs) of Breiðamerkurjökull, one of the largest outlet glaciers of the Vatnajökull ice cap, SE-Iceland, during its highstand of 1890 (LIA_{max}) and in 1945. The models were constructed by use of several sources: LiDAR DEM from 2010–2011, aerial and oblique aerial photographs, topographic maps from 1904 and 1945, written historical documents along with geomorphological field evidence. We estimate the retreat of the terminus as >5 km since the LIA_{max} to 2010, as a consequence of which ~114 km^2 of land has become exposed. Average annual loss of glaciated area amounts to about 0.95 km^2/yr to the year 2010. The period was divided into two intervals; 1890–1945 [55 yr] and 1945–2010 [65 yr]. The response is in accordance with climate changes and ice mass loss accelerated with increasing summer temperature. The total volume loss over 120 years is 69 ± 8 km^3 water equivalent (w.e.). This corresponds to an annual average specific mass loss of 0.64 m w.e./yr, 0.34 km^3 w.e./yr from 1890 to 1945 and 0.74 km^3 w.e./yr from 1945 to 2010. About 2/3 of the ice loss has occurred after the mid 20th century.*

2.1 Introduction

Breiðamerkurjökull ranks as the fourth largest outlet glacier of Vatnajökull ice cap, SE-Iceland. The outlet contains a blend of valley glaciers, heading off the ice covered eastern flanks of Öræfajökull central volcano and large ice streams flowing in between Máfabyggðir and Esjufjöll nunataks and from the relatively flat central field of Vatnajökull ice cap (Björnsson, 1996, 2009). Contemporary written descriptions over more than three centuries, along with geographical maps from various times, describe the dynamic behaviour of the outlet throughout the period, both during advance and recession. Scholars trace its advancing period back even to as early as late 14th century (Thoroddsen, 1931; Eyþórsson, 1952 a; Björnsson, 2009). The present day forefield, the Breiðamerkursandur delta (Figure 11), was at that time covered with vegetation but was gradually devastated during the climate deterioration of the Little Ice Age (LIA).

By the beginning of the 18th century the progressive advance had seriously affected utilisation of the farmland, and even destroyed it (Magnússon, 1955; Pálsson, 1945; Frisak, 1812; Henderson, 1957; Thoroddsen, 1931; Þórarinsson, 1943, 1956; Eyþórsson, 1952b). Continued advance of the glacier finally ruined the vegetated flat plain in the 18th century and overran farms, which had been evacuated decades before. Two maximal stages are recorded, first a highstand in 1750–1760 and second near 1880–1890. The advance in the 19th century led to the greatest late Holocene extent of the glacier (Þórarinsson, 1943; Björnsson, 2009).

Breiðamerkurjökull advanced 10–15 km during the LIA period (Tómasson & Vilmundardóttir, 1967; Björnsson, 1998, 1996; Björnsson & Pálsson, 2008). Glacier advances

are documented in the 18th and 19th centuries, including numerous surge events, especially in the eastern arm, Norðlingalægðarjökull (Pálsson, 1945; Frisak, 1812; Henderson, 1957; Thoroddsen,1931; F. Björnsson, 1998; H. Björnsson, 2009). No large scale dynamic instability occurred in the two major western arms. The terminus west of Esjufjallarönd had advanced to its maximum extent in 1870–1880 and remained there until 1890 (F. Björnsson, 1998). Written documents reveal that the terminus east of Jökulsá reached its maximum a little later or around 1890. A part of the eastern terminus was still advancing in 1894 (Þórarinsson, 1943; F. Björnsson, 1998) when a narrow gap (<250 m) separated the outlet from the coastline on the Breiðamerkursandur delta (Watts, 1962; F. Björnsson, 1998). Occasional local advances were witnessed close to the Esjufjallarönd medial moraine in the 19th and early 20th century while little change was observed east of the Jökulsá glacier river (F. Björnsson, 1998).

For simplification we reference the LIA_{max} extent as of the year 1890 because most of the terminus started to retreat slowly in the last decade of the 19th century. Contemporary statements testify that the shape of the terminus didn't change significantly from the LIA_{max} until it was surveyed in 1903–1904. Despite the recession had then just begun, temporary advances of parts of the terminus were observed (F. Björnsson, 1998). Even as late as 1982 the part closest to and west of the Esjufjallarönd medial moraine advanced (Rist, 1983). However, Breiðamerkurjökull has on the whole retreated throughout the 20th century to present time.

2.2 Previous work

Several geodetic surveys of Breiðamerkurjökull were carried out during the 20th century. First, in 1904 Öræfajökull and Breiðamerkurjökull were surveyed by the Danish General Staff (DGS). The resulting maps, published in 1905, were based on an analytical triangulation survey by the Generalstabens Topografiske Afdeling (Herforingjaráðið, 1905; Böðvarsson, 1996). The survey was carried out only 14 years after glaciers in Iceland had in general reached their maximum stage. Second, the U.S. Army Map Service (AMS) maps, published in 1948–1951, are based on aerial photographs taken in 1945–1946 (Böðvarsson, 1996). Third, in 2010–2011 a high resolution digital elevation model was produced by airborne LiDAR measurements (Jóhannesson et al., 2013; Jóhannesson et al., 2011). Moreover, a database produced by recent aerial photogrammetry has been accumulated by Loftmyndir ehf. Various satellite images have also been obtained (including SPOT and MODIS).

After the mid 20th century, various authors mapped the Breiðamerkursandur forefield and the terminus of the glacier, and even Esjufjöll nunatak range (Durham University Iceland Expedition, 1951; Young & Harney, 1951; Young, 1953; Lister, 1953; Price, 1968; Howarth & Welch, 1969a, 1969b; Price & Howarth, 1970; Price, 1982; Á. Böðvarsson, 1996; Evans & Twigg, 2002, 2000). Sigbjarnarson (1970) documented several geographical aspects of Breiðamerkurjökull including area and volume changes. His estimation were based on data prior to the 1970s. A wealth of other data have been collected that shed light on the dynamics, hydrology and the subglacial topography of Breiðamerkurjökull (Boulton, 1988; Björnsson, Pálsson & Guðmundsson, 1992; Björnsson, 1999, 1996; Björnsson, Pálsson & Guðmundsson, 2001; Evans & Twigg, 2002; Guérin et al., 2010). Radio echo sounding surveys carried out in 1991 resulted in DEMs of both the surface and the bed of the glacier, revealing a 25 km long and 300 m deep trench from Jökulsárlón lagoon towards the base of Esjufjöll nunataks.

2.3 Study area

The Breiðamerkurjökull outlet consists of three major arms separated by the prominent medial moraines of *Máfabyggðarönd* and *Esjufjallarönd*, each with a well defined accumulation area (Þ. Thoroddsen, 1959; Sigbjarnarson, 1970; Björnsson, 1996; H. Björnsson, 2009). The accumulation area of the *Máfabyggðajökull* arm is located by 2/3 in the eastern flanks of Öræfajökull and Hermannaskarð and 1/3 is located south and east of the Máfabyggðir cliffs. The central *Esjufjallajökull* glacier arm is in a wide valley between Máfabyggðir and Esjufjöll nunataks, here landmarked as Snæhettudalur. The eastern arm, *Norðlingalægðarjökull*, which contributes to more than half of the outlet, emanates from the central Vatnajökull ice cap (Figure 11).

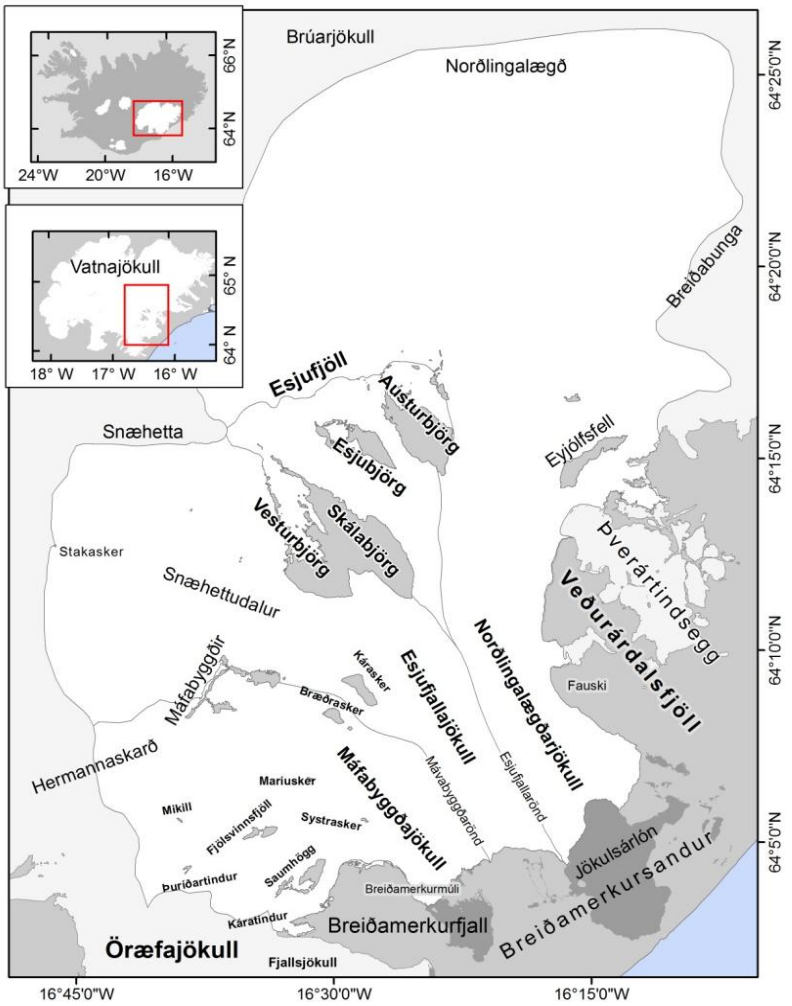

Figure 11. Breiðamerkurjökull outlet glacier of Vatnajökull ice cap, Southeast Iceland, and adjoining mountain ranges, Esjufjöll and Veðurárdalsfjöll. Ice divides (solid lines) of the three major arms.

The bulk of the ablation area rests in the broad valley between Öræfajökull and the Veðurárdalsfjöll mountains. The valley spans 11 km between Breiðamerkurmúli buttress in the west and the fell Fauski to east. The glacier's realm includes the ice-covered southern rim of the highland connecting Öræfajökull central volcano with Máfabyggðir and Esjufjöll range. Between Esjufjöll and Eyjólfsfell mountain a wide pass opens the rim where the Norðlingalægðarjökull outlet flows towards Breiðamerkursandur outwash plain, north from the ice divides at Brúarjökull and Norðlingalægð, hence the name of the glacier arm (Figure

11). The subglacial floor is more or less at an elevation of 100 m a.s.l. north to the foot of Esjufjöll (Jón Eyþórsson, 1952b; Björnsson, 1996).

Several smaller glacier branches merge to form each arm. The Máfabyggðajökull arm is composed of at least four outlets of Öræfajökull, separated by nunataks, medial moraines and ice divides. The Esjufjallajökull arm splits into two branches and the Norðlingalægðarjökull three (Table 7). Two great mountain ranges enclosed by ice are Esjufjöll nunataks and Veðurárdalsfjöll/Þverártindsegg to the east. Several small outlets emerge from these mountains, some adjoining the major glacier arms (Figure 12). Breiðamerkurjökull covered 906 km^2 in 2010, with the glaciers of Esjufjöll included. Adding up, the glaciers of Veðurárdalsfjöll mountains and Þverártindsegg covered about 28 km^2. In total Breiðamerkurjökull and adjoining glaciers thus covered about 939 km^2 in 2010.

Figure 12. Oblique aerial photo pointed southward above the Austurbjargajökull and Esjufjallajökull outlets, emanating from Mt. Esjufjöll range. The medial moraine of Esjufjallarönd (left) separates two of the major glacier arms of Breiðamerkurjökull. In distance the ice covered Öræfajökull central volcano (top right) but to left the Fauski in Veðurárdalsfjöll mountain range (Photo: SG, 16 August 2006).

2.3.1 Glacier terminus in 2010, lateral boundaries and ice divides

The present day terminus lies between Breiðamerkurfjall and Fellsfjall in Suðursveit district. Prominent end moraines mark its maximum extent on Breiðamerkursandur. In the bordering mountain slopes, lateral moraines, erratics, striated rocks and trimlines indicate the maximal stage and document the previous thickness of the glacier. In the ablation area, these landforms are obvious but they become more sparse and obscure in the accumulation zone.

Depicted from the LiDAR DEM the ice divide trends northwest from Antafjall crossing Hermannaskarð pass, north towards and across Norðlingalægð depression, about 15 km north

of Esjufjöll mountain, before turning south to the Breiðabunga glacier dome and adjoining outlet glaciers in Suðursveit (Figure 11).

2.3.2 Marginal mountains and nunataks

Several peaks in Breiðamerkurfjall, between Fjallsjökull and Breiðamerkurjökull, most of them unnamed, rise near the glacier margin. The first one's bordering the ice divide are Antafjallstindur and Káratindur peaks. North from there the outlets of Öræfajökull enshroud the flanks with few obtruded nunataks. Highest are Heljargnípa og Þuríðartindur. Saumhögg forms the base of the Heljargnípa ridge. North of it is the Fjölsvinnsfjöll ridge. The last striking nunataks observed in the eastern flanks of Öræfajökull is the cliff Mikill. Veðurárdalsfjöll and Þverártindsegg mountains border the eastern margin of Breiðamerkurjökull. Among these the nunatak Eyjólfsfell (915 m) is found to the north. In all of those bordering mountains and in numbers of nunataks, lateral moraines, erratics and striated rocks are observed.

The Máfabyggðir and Esjufjöll mountains are the largest nunataks within the border of Breiðamerkurjökull outlet. The 4 km long cliffs of Máfabyggðir are of rhyolitic and basaltic origin. Esjufjöll consists of four pararell mountain ridges from the glacial covered Snæhetta mountain (1745 m). Respectively from west to east are: Vesturbjörg, Skálabjörg, Esjubjörg og Austurbjörg. A multitude of small peaks rise from the long ridges. The narrow Fossadalur valley is located between the dominant ridges of Vesturbjörg and Skálabjörg. It is now occupied by a glacier dammed lagoon (Fossadalslón, 0.9 km^2 in 2010) and the valley glacier Fossadalsjökull. Snæhetta is an about 15 km long crest outlining the highest part of the Esjufjöll range. The highest glacier dome on the crest is about 4.5 km west of Vesturbjörg. Esjubjörg and Austurbjörg are the easternmost of the four dominant mountain ridges but this part of the Esjufjöll range and the northern interior of Breiðamerkurjökull glacier was not mapped by the DGS in 1904.

2.3.3 Nunataks and rocky outcrops exposed in the 20th century

Several previously subglacial peaks became visible as nunataks as a consequence of glacier recession during the 20th century. These bring important clues on surface elevation at past times as the lowering can be traced from aerial photographs of 1945 and the derived AMS maps series. Nunataks (chapter 2.3.2) rising at higher elevation in the accumulation area, were not submerged within the study period. Many mountain peaks and rock outcrops in the lower reaches of the accumulation zone and ablation zone were all covered by ice at the end of the 19th century. Evidently none of them was exposed on the 1904 maps but the location of a few survey points on the glacier surface can be identified where later nunataks emerged and therefore give an indication about the former ice thickness. Largest of those are Bræðrasker, Kárasker, Systrasker og Maríusker, south of Máfabyggðir and Esjufjöll (Figure 11 and 13). A few rocky outcrops can be spotted in the wide Snæhettudalur valley, the highest of them at an elevation of 1600 m in the southern flanks of Snæhetta (Figure 13). Six small outcrops representing subglacial ridges protrude through the the glacier surface. Rock outcrops and nunataks are now exposed on the eastern part of the Esjufjöll crest and northwest of Eyjólfsfell, having been covered by the glacier until the late 20th century.

Figure 13. Bræðrasker (left above center) and Kárasker (the larger nunatak) were covered with ice until the 20th century. Local habitants assume the latter was exposed sometimes between 1930–1940 in a period of rapid thinning (S. Björnsson, 1957). Bræðrasker was exposed near 1960 (S. Björnsson, 1979). The Máfabyggðir nunataks (above Bræðrasker) and a tiny rock outcrop in lower Snæhettudalur valley can be seen in the distance near to the right, just left of Vesturbjörg in Esjufjöll (Photo: SG, 17 August 2006).

2.4 Data acquisiton

Our basic data base describing the glacier geometry contains: a) LiDAR DEM from 2010–2011 b) georectified aerial images from August 2003 from Loftmyndir ehf©, c) oblique aerial photographs from 2006, 2011 and 2012, d) in situ GPS 2011 and 2012 tracking of geomorphological features outlining the LIA_{max} extent of the glacier, e) topographic maps 1904 and 1945, f) aerial photographs of the AMS series, 30th of August 1945 and September 1946, g) MODIS images from 2002 to 2013. h) SPOT-5 images.

2.4.1 LiDAR, aerial photographs and satellite images

The airborne LiDAR mapping of Breiðamerkurjökull was carried out in August 2010 and September 2011 (Jóhannesson et al., 2013). The main product has 5x5 m horizontal resolution but a 2x2 m high resolution DEM of Esjufjöll and Máfabyggðir was calculated from the point cloud for this project. The LiDAR DEMs were also used as shaded relief for constraining present day (2010) glacier extent in Esjufjöll and Máfabyggðir. The vertical accuracy is within 0.5 m, providing precise elevation of geomorphological remnants of the LIA_{max}.

The Loftmyndir ehf© database offers high resolution aerial photographs of the mountainous field surrounding Breiðamerkurjökull, Öræfajökull and Þverártindsegg. The database neither covers Esjufjöll and Máfabyggðir nor most of the nunataks. These photos were taken in August 2003 from an elevation of 3500 m. They are originally taken on film and then

digitally scanned (Loftmyndir ehf©, 2010). With resolution of 0,5 m/pixel this database was very useful to identify various geomorphological features.

The aerial photographs of the AMS series, were taken on 30th of August 1945 and in September 1946 from elevation of 7000 m (Army Map Service, 1950). The original films are lost but digital scanned copies provide fair resolution but limited contrast range. They cover nearly all the area within the boundary of Breiðamerkurjökull and most importantly, every nunatak and rock outcrop exposed in 1945–1946, about 55 years after the LIA_{max}.

An oblique aerial photograph, taken from the airship Graf von Zeppelin on 17th of June 1930, shows the eastern part of the Breiðamerkurjökull towards Fellsfjall mountain. In the forefront is the now extinct river Stemma. The surface shape of the glacier, 40 years after its maximum extent, can be examined from the photo.

Oblique aerial photographs for helping to delineate the LIA_{max} extent were taken by the author (SG) on 16th and 17th of August 2006. They cover most of Breiðamerkurjökull and surrounding mountains including nunataks and rock outcrops. They were digitally scanned from 35 mm and 6x7 medium format films.

By use of SPOT-5 images, along with LiDAR DEM, individual glacier branches of the Breiðamerkurjökull were delineated. Estimates of the elevation of the present day snowline where derived from MODIS images from 2002 to 2013 (MODIS, 2013). Images, usually taken in September and selected when no new snow covered the accumulation area, were downloaded and imported into ArcGIS.

Data of the subglacial topography of Breiðamerkurjökull were provided by the Jöklahópur (the glacier group) of the Institute of Earth Sciences, University of Iceland. These were obtained by radio echo sounding surveys in 1991 (Björnsson, Pálsson & Guðmundsson, 1992; Björnsson, 1998, 1996, 2009).

2.4.2 The 1904 DGS maps

Four maps of the DGS, in a scale 1:50 000 and with 20 m contours, cover large part of Breiðamerkurjökull and Öræfajökull. The lowland was surveyed in 1903 and Öræfajökull and Breiðamerkurjökull in 1904. Numerous survey points were located on the glacier surface and near the margin (Böðvarsson, 1996; Herforingjaráðið, 1905). The numbered map sheets are:

87 NA Öræfajökull – Esjufjöll. Covers northern Öræfajökull central volcano, Máfabyggðir og western part of Esjufjöll range and Breiðamerkurjökull outlet glacier.

87 SA Öræfajökull – Hvannadalshnúkur. Covers Öræfajökull at large, including Fjallsjökull, Breiðamerkurfjall mountain and western area of Breiðamerkurjökull.

97 NV Kálfafellsstaður – Reynivellir. Eastern part of Breiðamerkurjökull and Þverártindsegg mountain.

97 SV Kálfafellsstaður – Hrollaugseyjar. Southeast part of Breiðamerkurjökull where Jökulsárlón lagoon is presently sited and Breiðamerkursandur plain as a coastal strip.

Sheets no 86 and 96 cover Norðlingalægð and Breiðabunga, respectively were published in 1944, based on aerial photographs from 1937–1938. They belong to the *Atlas* series of maps

in scale 1:100 000. The sheet no 86 (Vatnajökull) has great deviations compared to the LiDAR DEM due to lack of good landmarks in the ice cap's centre. The no 96 sheet (Hoffellsjökull) was referenced to greater accuracy but still has considerable horizontal errors on the Breiðabunga summit dome.

2.4.3 the 1946 AMS maps.

The six maps of the AMS C762 series were produced in 1949 and published in 1950–1951. The map scale is 1:50 000 with 20 m contours. The numbered map sheets are:

6019 I Veðurárdalsfjöll. Veðurárdalsfjöll og Þverártindsegg range, Esjufjöll and Breiðamerkurjökull.

6019 II Breiðamerkurjökull. Southern part of Breiðamerkurjökull, Breiðamerkurfjall og Veðurárdalsfjöll.

6019 III Öræfajökull. Northern Öræfajökull, Máfabyggðir and Breiðamerkurjökull.

6019 IV Esjufjöll. Western part of Esjufjöll and northern Breiðamerkurjökull.

6020 II Vatnajökull II. Breiðabunga glacier dome and northern Breiðamerkurjökull.

6020 III Vatnajökull III. Wast area of Breiðamerkurjökull north of Esjufjöll.

The AMS maps are fairly accurate in the horizontal coordinates when compared to the LiDAR DEM but the elevation shows unrealistic deviation in several places. Insufficient data, caused by clouds and lack of reference points due to little contrast in the interior of the Vatnajökull ice cap, prevented completion of stereo processing. The contours presented on the maps of those areas is based on the 1937–1938 oblique areal photographs, interpreting the surface form rather than showing the true elevation (Á. Böðvarsson, 1996).

2.4.4 Field studies

Remnants of glacial morphological features were located in several field trips. They outline the earlier extent of the glaciers but are, in numbers of places, poorly visible by remote sensing. They were not dated to verify exact age but could be traced outward to the prominent end moraines on Breiðamerkursandur delta and their continuing lateral moraines in Breiðamerkurfjall and Veðurárdalsfjöll. They outline the maximum glacier extent during the LIA as confirmed by contemporary sources.

Where inaccesible, site elevation and location was measured from safer ground. The method: a) GPS datapoint taken on site where the object was surveyed from, b) instrument height (TruePulse rangefinder) above ground noted and added to the altitude of the site (H), obtained later from LiDAR DEM, c) the angle ($\alpha°$) to object, slope distance, horizontal (D) and vertical distance measured. The height (z) of object above site elevation then calculated: $z = H + D \cdot \tan \alpha°$.

Field work was done in 2011 and 2012. The Innri-Veðurárdalur valley was visited in early June 2011. The geomorphological evidence of the LIA maximum is sparse but some features were noticed on aerial photographs. On the 1904 map by the DGS, the Breiðamerkurjökull glacier branch filled the valley floor, merged with Innri-Veðurárdalsjökull, which flows from

Þverártindsegg mountain. This dynamic environment involves steep scree slopes surrounding the narrow, glacier dammed sidevalley, that quickly had eroded LIA traces. Also noted were moraines, erratics and trimlines on the mountainsides of Fellsfjall, Fauski and Prestfell (Figure 14a, b).

In late July 2011, the Breiðamerkurmúli and Saumhöggsdalur valley were examined. As seen on aerial photographs, lateral moraines are intermittent in the northern side of the mountain and this makes it difficult to constrain them accurately. By field investigation we successfully managed to link those with other remnants such as erratics and chains of boulders (Figure 15a). The 1904 map shows the north side as glaciated but no field evidence supports this. Periglacial small-scale solifluction lobe landforms occur in the slopes up to an elevation of 740 m. These signs most likely indicate permafrost, frost heaving and are found in many places in the mountains surrounding Breiðamerkurjökull, as Innri-Veðurárdalur and in Esjufjöll (Dabski & Angiel, 2010). The eroded slopes of Saumhögg and Fjölsvinnsfjöll were inspected as much as possible from distance but they show various signs of the earlier LIA_{max} glacier surface.

The Hrossadalur valley in Breiðamerkurfjall (Figure 15b) was visited in early April 2012. Breiðamerkurjökull and Fjallsjökull remained merged together there until 1946 (F. Björnsson, 1998). Erratics and moraines are poorly visible from aerial photographs but they were verified and tracked in the field. According to the 1904 map the glacier dammed the valley mouth at the altitude of 95 m but erratics observed in the field show that it has reached an elevation as high as 145 m. Signs of the glacier extending into Hrossadalur are obvious and there are indications of two stages of advance.

A field trip to Máfabyggðir and Öræfajökull was carried out in April 2012 and to the Esjufjöll range in June (Figure 16a, b). The LIA_{max} extent was outlined in several places in the range such as around Máfabyggðir cliffs. Attention was given to nunataks in the accumulation area. Amongst them a modest nunatak obtrudes at the ice divide about 12 km north of Hermannaskarð (landmarked as Stakasker,1492 m.a.s.l, see Figures 11 and 17a). It is visible on the 1945 aerial photographs so it serves as an important signpost of elevation changes in the accumulation area. In Esjufjöll and Máfabyggðir, a wealth of geomorphological evidence was identified to outline the LIA_{max} extent in that area. Some have previously been identified and dated (Dabski & Angiel, 2010).

The shallow side valley, Fremri-Veðurárdalur was visited in July 2012 for studying how firmly the lateral margin could be traced. Remnants shows that the glacier surface has lowered as much as 240 m since its maximum stage (Figure 17b). This observation is in accord with information from local inhabitants (Fjölnir Torfason, personal communications, 27 March 2014).

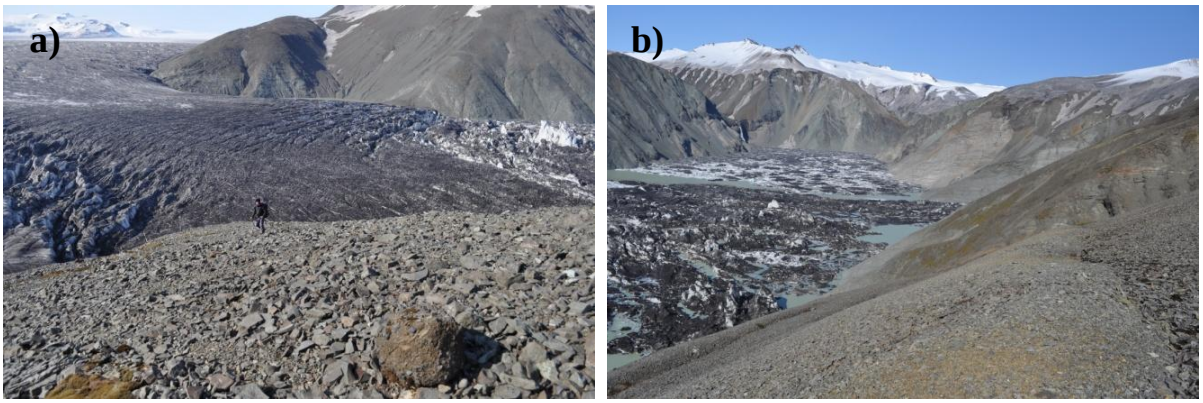

Figure 14. LIA remnants in Fauski mountain. a) Erratic and b) lateral moraine in Innri-Veðurárdalur. These remains are about 120 m above present glacier surface (Photos: SG, 3 June 2011).

Figure 15. Geomorphological LIA$_{max}$ remnants in Breiðamerkurfjall mountain. a) Lateral moraine in northern slopes of Breiðamerkurmúli (Photos: SG, 28 July 2011). b) Glacier erratics spotted in Hrossadalur valley (Photo: SG, 4 April 2012).

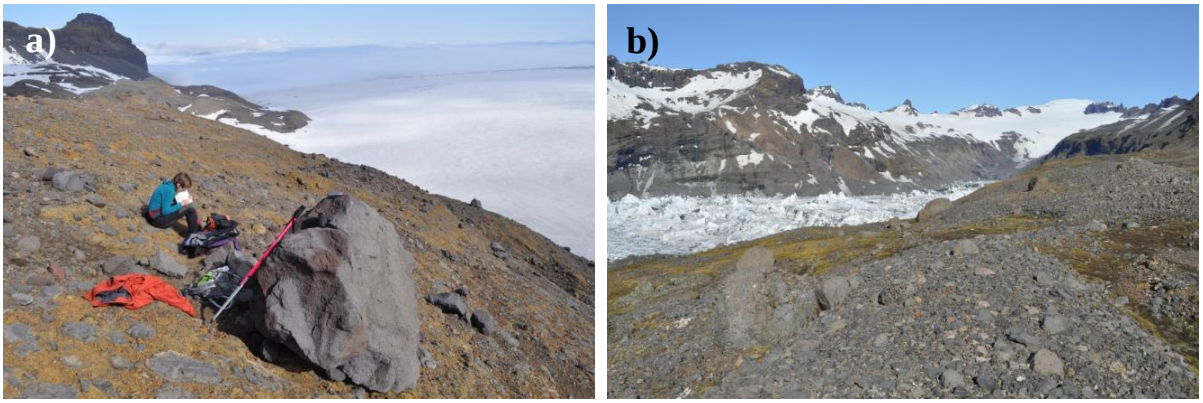

Figure 16. LIA remnants in Esjufjöll mountain range. a) Erratic in Vesturbjörg >60 m above present glacier surface at an altitude of 930 m. b) lateral moraine in Fossadalur valley. (Photos: SG, 3 June 2012).

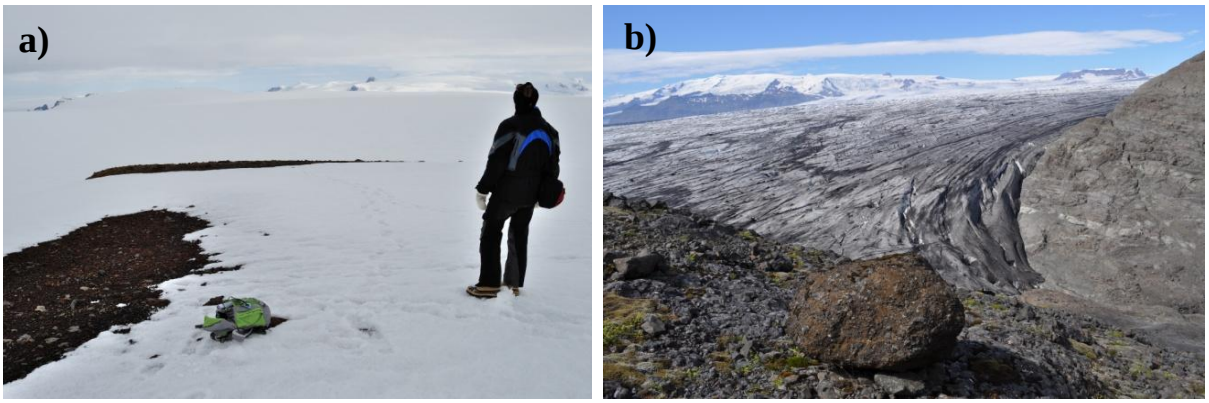

Figure 17. a) View towards Hermannaskarð from the nunatak Stakasker (Photo: SG, 4. June 2012). b) Erratics in Fremri-Veðurárdalur, 200 m above the present surface (Photos: SG, 11 July 2012).

2.5 Reconstruction of Breiðamerkurjökull

The delineation of the extent of Breiðamerkurjökull at LIA_{max}, 1945 and 2010 was largely based on remote sensing. DEMs of the surface geometry in ~1890 and 1945 were constructed in ESRI ArcGIS and Surfer based on the geomorphological evidence described above and the contours of the AMS maps and partly the 1904 maps.

2.5.1 The 2010 DEM and ice margin

The LiDAR DEM served as a reference. Ice divides were determined from the DEM but lateral boundaries using the DEM as well as the Loftmyndir ehf© database. The Esjufjöll and Máfabyggðir range along with nunataks were digitized to delineate the glacier area as accurately as possible. Where controversial, the delineation was done by comparison with oblique aerial photographs.

2.5.2 Ice divides

Ice divides were assumed to remain the same during the time period 1890 to 2010 (in lack of better data), which introduces a possible error in the areal extent, in particular because the surges of Brúarjökull (1890 and 1963–1964) and Eyjabakkajökull (1890) may have caused shifts of ice divides (Björnsson et al., 2003). How much effect this would have on the total volume estimates presented here is hard to assess, but near the ice divides the thickness changes have probably been relatively small compared to those of the terminus and in the ablation area. At high elevations on Öræfajökull and in large areas within the interior of Vatnajökull ice divides are well defined by mountain ridges.

2.5.3 The LIA_{max} ice margin

The terminus and lateral boundaries were digitized in the centre of the end moraines and the various geomorphological landforms. The Loftmyndir ehf© database was very useful during this procedure due to its high resolution. On the Breiðamerkursandur delta remnants are easily recognizable and can be traced up to 760 m in Veðurárdalsfjöll mountains and >600 m in Breiðamerkurfjall mountain. At higher elevation they become sparse and disappear in the accumulation zone. Some could be traced higher up at several sites and as high as ~1100 m in Esjufjöll range.

Gaps in the outline where lateral moraines could not be identified were filled in by interpolation between the nearest identifiable marks on each side. The interpolation was carried out in the elevation as an indipendent variable and based on the LiDAR DEM.

2.5.4 The LIA_{max} ice surface

The construction of the 1890 DEM was based on three different elevation models; the 1904 DGS maps, the 1945 AMS map and the 2010 LiDAR DEM. The maps of 1904 and 1945 have some shortcomings. The DGS map of 1904 does not describe the true LIA_{max} ice margin, as determined by the modern remote sensing and in situ field work. Moreover, the map is in error in several areas in the upper reaches. Further, the upper part of the glacier on the AMS 1945 maps is based solely on an elevation model produced from oblique photos taken in 1937–38. Nonetheless the maps of 1945 and 1904 outline a similar general shape of the glacier as the 2010 map. A detailed comparison of the aerial photographs from 1945 side by side with the LiDAR DEM show the same glacier surface features despite the 65 years time interval (Figure 18a-b). This fact forms the basis for our reconstruction of the 1945 and 1890 maps.

Throughout the post-LIA period the glacier basal topography has been covered by a thick glacier with a smooth surface. This applies both for the lower part of the glacier which is underlain by a flat plain and the upper part flowing over sloping bed (Björnsson, 1996). An exception is a few areas around recent outcrops in the ablation zone that were totally hidden by ice in 1945, as observed in aerial photographs. The glacier terminus has retreated by up to 4 km over the 65 years since then but keeps approximately its parabolic shape, as can be observed on longitudinal profiles (see Results section).

When reconstructing the ice surface of 1945 and the LIA_{max}, the contour lines were drawn across the glacier assuming that they are parallel with the 2010 LiDAR DEM contours. First, the elevation difference between the LIA_{max} and the 2010 ice surface was estimated in a number of carefully chosen points along the ice margin. A least-squares relationship between the 2010 LiDAR and the LIA_{max} ice surfaces was used to estimate the surface lowering as a function of elevation from 480 m to 1560 m a.s.l. (Figure 19). Above this interval the geomorphological evidence indicates very little change in ice surface elevation as was also found in an analysis of ice surface elevation in neighbouring Kotárjökull in Öræfajökull (Guðmundsson et al., 2012). The least-squares relationship was used to raise the LiDAR data (using Surfer). The resulting grid was then imported into ArcGIS and used to create contours with 20 m spacing. These contours were modified near the glacier margin to meet the adjoning contour lines on the LiDAR DEM on ice-free land. The contours were then imported again into Surfer where a new grid was created.

Second, in the altitude range 250 to 480 m a.s.l., the LIA_{max} DEM was derived by shifting the contours from the 1945 AMS maps vertically using an elevation change that led to a smooth LIAmax ice surface at 480 m a.s.l. Over this narrow elevation range the difference in altitude between 1890 and 1945 may be assumed to be the same within the uncertainty of this analysis. These contours were digitized manually and merged with the modified LiDAR DEM.

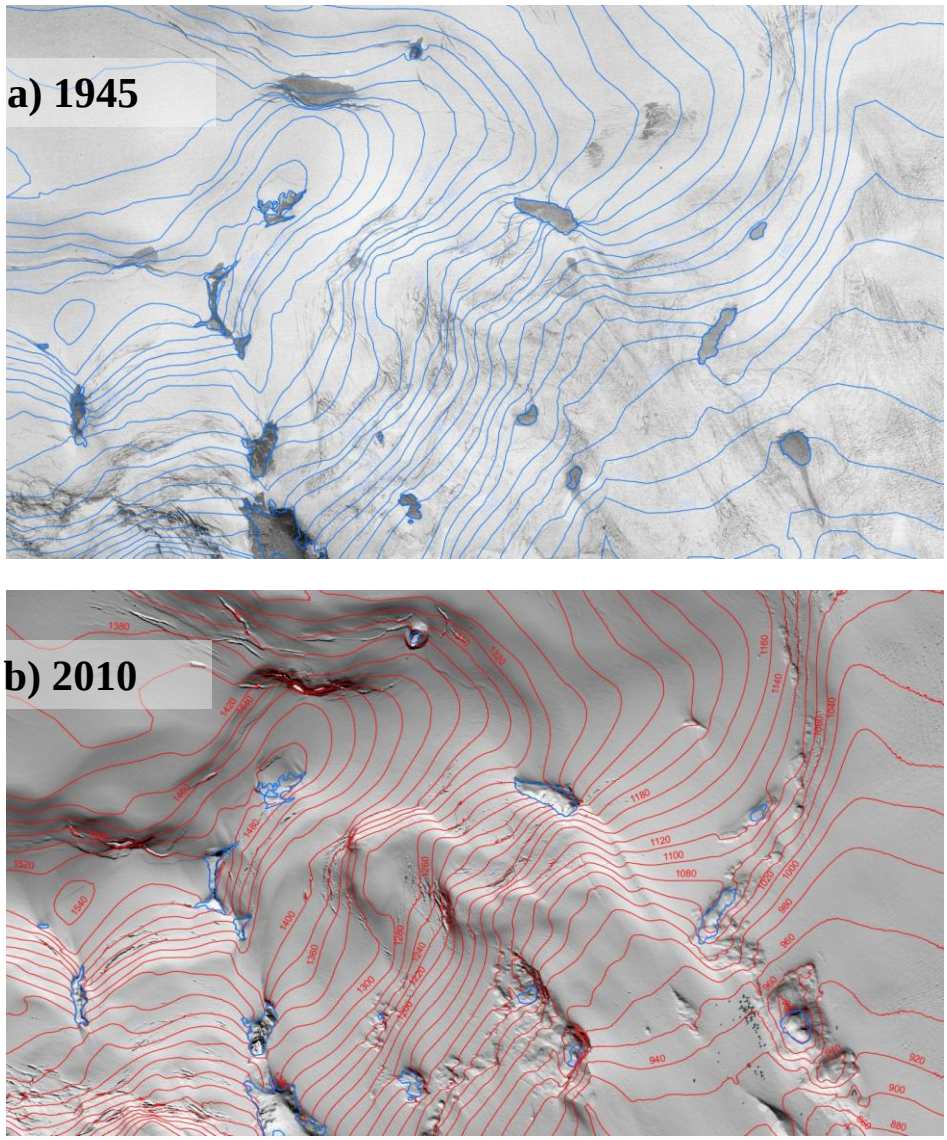

Figure 18. The eastern part of Esjufjöll mountains in a) 1945 and b) 2010 from 880 m (lower right corner) to 1540 m altitude. Surface changes diminish gradually upslope. The blue curves (both photos) represents the 1945 ice margin. Exposed rock outcrops at higher altitude were similar in size in 2010 as in 1945. Downslope, however, the nunatak were more exposed in 2010.

In the lowest part of the terminus, below 250 m, the LIA_{max} DEM was based on the contours of the 1904 DGS DEM which can be regarded as a fairly accurate description of the shape of the termini (Figure 20) despite the slight retreat up to 1904. Some minor adjustment were made near the ice margin based on the geomorphologically determined LIA_{max} margin position.

As a test of the reconstructed LIA_{max} DEM we refer to a late 19^{th} century report that the forefront of Esjufjallarönd had reached such heights to obstruct the view towards east to the Borgarhafnarfjall mountain in Suðursveit district from the farm Kvísker in Öræfi district, about 40 km to the west (F. Björnsson, 1996). Line-of-sight inspection indicated that the terminus had to rise approximately 120 m above surrounding land to hide this mountain. This is in good accordance with our elevation model. The LIA_{max} terminus was compared to the 1904 maps to verify the contemporary sources claiming that Breiðamerkurjökull had retreated ~100–200 m at time of the DGS survey, and this turned out to be the case (Figure 20).

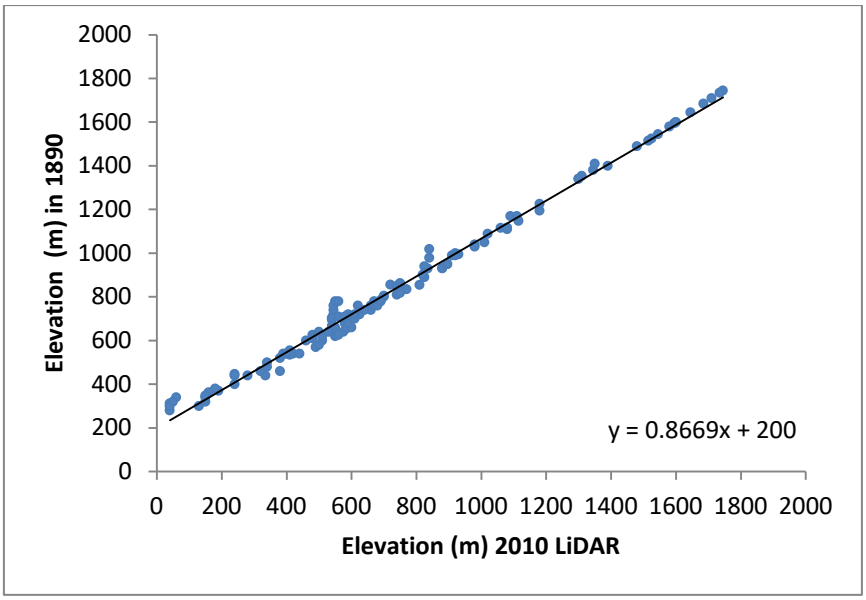

Figure 19. Glacier surface elevation along the lateral margins of Breiðamerkurjökull at LIA_{max} and 2010. Changes in glacier elevation are largest near the terminus and diminish gradually to near zero above 1560 m. A least-square linear relationship was used to raise the 2010 surface without changing its shape in the altitude range of 480 to 1560 m (see text for explanation).

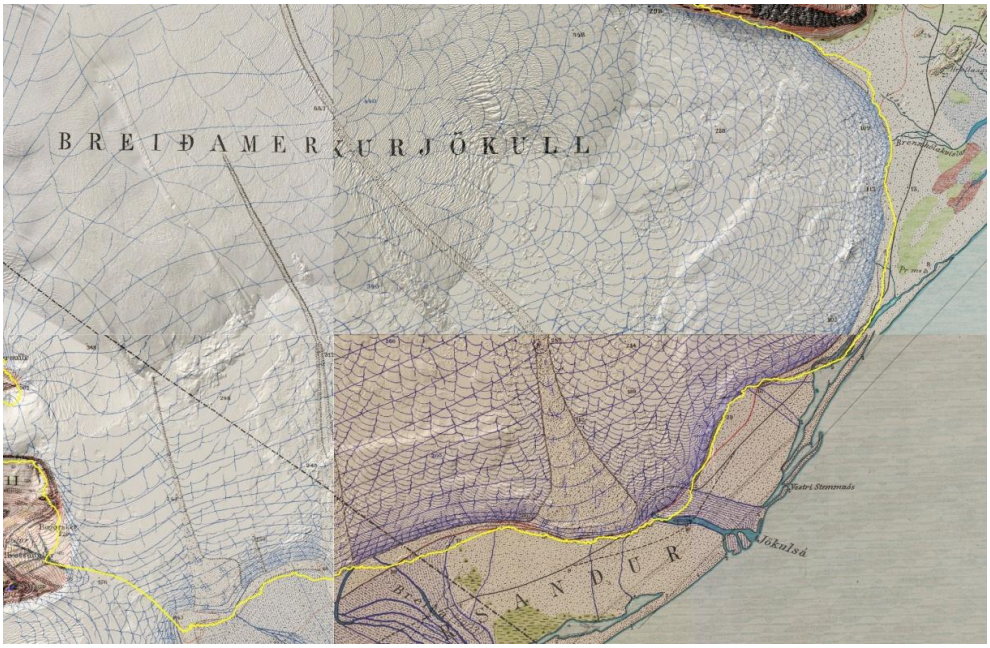

Figure 20. Comparison of the DGS 1904 and the LIA_{max} glacier extent (yellow line, traced from LiDAR) terminus shows the retreat of the glacier margin in the period 1890–1904. Along the terminus the glacier had retreated about 100–200 m in 1904 but somewhat less near the medial moraines. The maps are represented with minor transparency to show prominent land features on Breiðamerkursandur delta.

Further, elevation points, measured on the glacier surface in the 1904 DGS survey, were compared with the LIA_{max} surface model to assess accuracy. The exact location of several points is somewhat speculative as no well-defined surface characteristics can be identified. Despite the uncertainity this leads to hints about the elevation. Several points can be firmly identified, some near the lateral margins but other became exposed later as nunataks (Figure 21). Some flaws in the 1904 maps were obvious, especially near unidentified elevation points.

This can be explained as measurement errors or misplaced survey points. Well identified points, however, showed little deviation. Hence, we conclude that the surface elevation remained more or less the same in 1904 as at the LIA_{max}.

The error of the estimated LIA_{max} ice surface elevation and derived ice volume changes since 1890 is hard to estimate quantitatively but a partly subjective assessment can be provided by roughly estimating the error of the different data sources that were used to derive the LIA_{max} DEM. The purpose is not to estimate the local error of individual points in the DEM, which can be variable and is highly affected by outliers in the geomorphological data or historical maps but rather a large-scale error or bias that will affect estimates of ice-volume changes for the whole or large parts of the ice-flow basin.

Four sources of error need to be considered for altitudes >480 m a.s.l. where the LIA_{max} DEM was derived by shifting the 2010 LiDAR DEM vertically based on geomorphological evidence of the LIA ice margin. 1) The elevation error in the 2010 LiDAR DEM is <0.5 m (Jóhannesson et al., 2013, 2011). This is much less than other sources of error and has negligible effect of the final error estimate. 2) Available data from nunataks show that the change in the ice surface elevation between 1945 and 2010 above 1560 m a.s.l. is near zero with a standard deviation of 5 m. As changes from 1890 to 1945 at the highest altitudes may be assumed to be smaller than from 1945 to 2010, this indicates that little change has taken place at these altitudes since 1890. This is consistent with elevation changes <5 m from 1891 to 2010 at 1677 m a.s.l. for Kotárjökull in Öræfajökull (Guðmundsson et al., 2012). Furthermore, the trend with altitude of the changes in the ice surface elevation below 1560 m a.s.l. (Figure 19) clearly indicates an approach to near zero at the highest altitudes. The standard error in the estimated LIA_{max} ice surface elevation above 1560 m a.s.l. (80 km^2) is here roughly estimated as ±5 m based on these indications. 3) The altitude of the LIA ice surface near the lateral margins, estimated from geomorphological evidence, is considered to be accurate to ±5 m. 4) The estimate of the ice surface elevation in the interior of the glacier derived by vertical shifting of the 2010 DEM assumes that the glacier had the same geometrical shape in 1890 as in 2010. This assumption brings in additional uncertainty which is here assumed to lead to total uncertainty of ±10 m in the range 480–1560 m a.s.l. (800 km^2).

Below 480 m a.s.l., the LIA_{max} ice surface is estimated from the contours of the AMS and DGS maps, above and below 250 m a.s.l., respectively. The AMS contours from 1945 were shifted vertically based on geomorphological evidence to account for the lowering of the glacier surface since 1890, assuming that the glacier had the same geometrical shape in 1890 as in 1945, but the DGS contours from 1904 were assumed to represent the 1890 ice surface elevation within the accuracy of the analysis presented here and were therefore not shifted. The error in the DGS map may be quantitatively estimated from peaks and survey points in the bordering mountains because similar errors should be expected on the glacier surface as in the the bordering mountains in this elevation range. Elevation of such points were collected and compared with the corresponding elevations interpolated from the LiDAR DEM showing elevation biases ranging from 4–14 m, with an RMS of 6 m (Appendix A). In order to account for the small change in the ice-surface elevation may have taken place from 1890 to 1904, the accuracy of the LIA_{max} DEM below 250 m a.s.l. (55 km^2) is conservatively assumed to be within ±10 m. The accuracy of the AMS map may be assumed to be better than for the DGS map because the underlying aerial photographs and stereographic processing should lead to smaller errors. The uncertainty of the LIA_{max} DEM for altitudes in the range 250–480 m a.s.l. derived from the 1945 AMS map (55 km^2) is nevertheless again estimated to be ±10 m

because of the additional error associated with the the vertical shifting to account for the lowering of the ice surface between 1890 and 1945. Thus, the large-scale error or bias of the LIA_{max} DEM is estimated as ±10 m for the entire area below 1560 m a.s.l. but somewhat smaller above this altitude where changes of the ice surface elevation are assumed to have been near zero since 1890.

Assuming statistically independent errors in the above four elevation ranges, $z<250$, $250<z<480$, $480<z<1560$, and $z>1560$ m a.s.l., the total error in the estimated ice-volume change for the period 1890 to 2010 for the whole ice flow basin can be calculated as the RMS value of the individual error components, which amounts to ±8 km^3 water equivalent. As the error sources are more or less of similar nature and magnitude in the following section on the 1945 ice surface DEM, the same error estimate may be assumed for the estimated ice-volume change for the period 1945 to 2010.

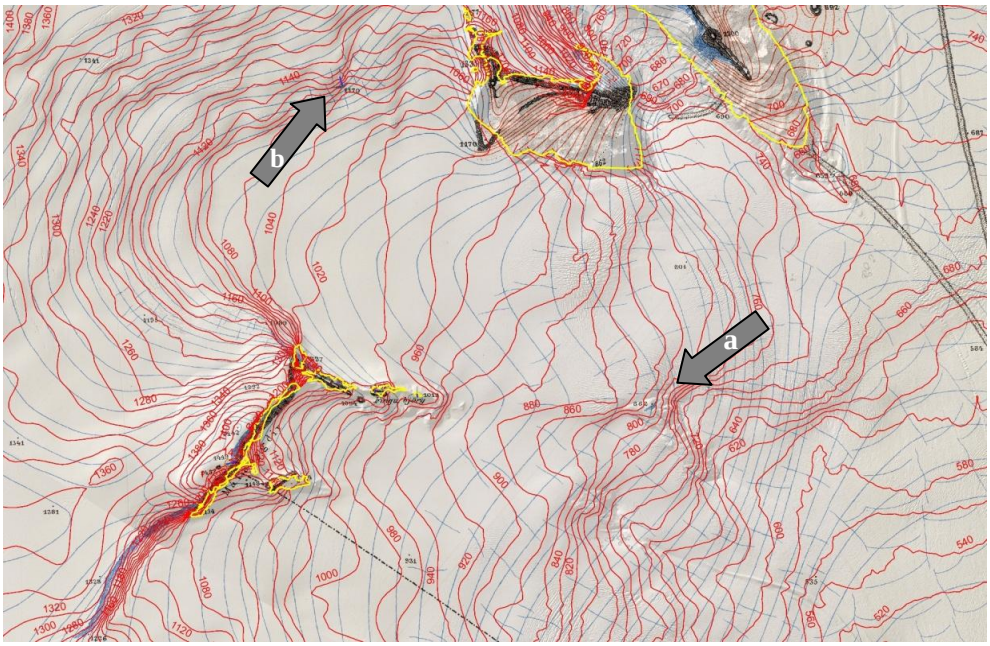

Figure 21. An example to demonstrate the credibility of the 1890 DEM. Composition of LiDAR DEM (base), overlying semitransparent DGS 1904 map and LIA_{max} contours (red). LIA_{max} ice margin marked yellow. The Kárasker nunatak (a) was ice-covered when the area was surveyed in 1904 but a crevasse bulge at 862 m a.s. l. coincides with it. The resulting LIA_{max} contours show similar altitude. An crevasse bulge, in Snæhettudalur (b) measured 1170 m in 1904 coincide with 1100 m outcrop exposed in the late 20th century. The model predicts 1160 m.

2.5.5 The 1945 ice margin

The 1945 outlines were delineated from the original aerial photographs and the LiDAR DEM instead of relying upon the published AMS maps. The maps lack details of the glacier margin across the forefield. Therefore the original scanned photographs were georeferenced in ArcGIS as accurately as the resolution allowed with respect to the LiDAR data. The lateral boundaries and the terminus were then digitized. The AMS maps didn't match with the aerial photographs in a few places. As an example occasional shadows crossed the glacier lateral boundaries but had on the maps been interpreted as cliffs. The resolution and contrast of the photographs didn't always allow clear rendering of the lateral boundaries in shadows. To solve such uncertainity, the ice margin below and above such sites was digitized and the unclear margins estimated as described in 2.5.3.

2.5.6 The 1945 ice surface

The elevation contours of the AMS 1945 maps has by some earlier researcher been regarded as fairly accurate up to elevation of about 900 m as they were produced by stereo photogrammetry. They were therefore used initially for the construction of the 1945 DEM. This worked convincingly to begin with but problems were encountered at about 600 m elevation as each contour line needed large modifications to meet adjoing ones on land in the LiDAR DEM. Therefore, instead of continuing using the AMS maps, the surface above 600 m was reconstructed by modifying the LiDAR DEM, with the same method as explained in 2.5.4. The thickness changes between 1945 and 2010 were measured as described above, an average linear trend calculated and then imported to Surfer to modify the LiDAR data to derive the 1945 DEM (Figure 22).

Nunataks and rock outcrops above about 1300 m seem mostly similar in 2010 as in 1945, but the ice surface lowering can be estimated from few sparsely distributed outcrops of rocks. Below 1300 m, thickness changes from 1945 to 2010 are clearly revealed on nunataks and outcrops, increasing downwards in the ablation zone. A number of outcrops added valuable information about thickness changes, some partly or totally hidden in 1945 but now visible. In the ablation area thickness changes since 1945 are easily estimated along the lateral margins, increasing gradually down-glacier and reaching about 180 m near the present terminus.

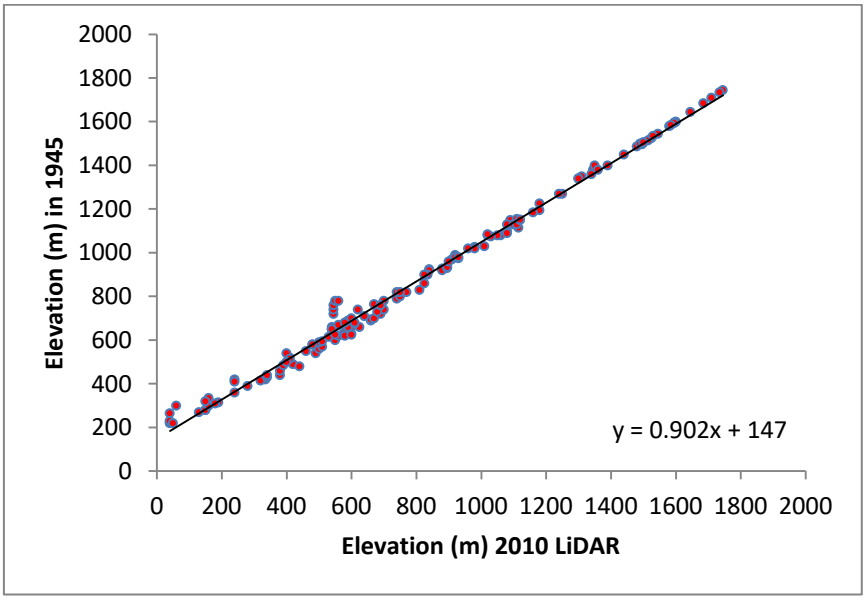

Figure 22. Glacier surface elevation along the lateral margins of Breiðamerkurjökull in 1945 and 2010. The margin elevation was estimated from the 1945 aerial photographs and the LiDAR DEM of 2010. A least squares linear relationship was then used to raise the 2010 surface.

2.6 Results derived from DEMs

We use the derived DEMs to describe the various brances of Breiðamerkurjökull from their LIA maximum extent to the present, their changes in elevation, area and volume.

2.6.1 Demarkation of glacier branches

By use of the LiDAR DEM and SPOT–5 images, individual glacier branches were traced by surface characteristics and their 2010 area estimated. Table 7 compiles various charateristics of the branches (Figure 23).

Table 7. The present day (2010) Breiðamerkurjökull and adjoining valley glaciers. Individual glacier branches (column 1), centre lines and ice divides. Elevation of ice divide or head of the glaciers (col. 2) and snouts (col. 3), the length of each stream (col. 4) and area size (col. 5). Bold numbers gives the total for each of the major branches and mountain area.

Glacier branches (in 2010)		**Head$_{(m)}$**	**Snout$_{(m)}$**	**Length $_{(km)}$**	**Area $_{(km2)}$**
Máfabyggðajökull – Western arm					**146**
i.	*Saumhöggsjökull*	1540	100	7.9	7
ii.	*Heljargnípa – Fjölsvinnsfjöll*	1900	40	14.4	27.5
iii.	*Öræfajökull – Hermannaskarð*	1770	20	21.2	73
iv.	*Máfabyggðir – Kaplaklif*	1400	20	19.7	39
Esjufjallajökull – Central arm					**203**
v.	*Máfabyggðir N – Snæhetta*	1745	20	31.0	161
vi.	*Vesturbjargajökull*	1740	20	29.2	42
Esjufjöll mountains					**58**
vii.	*Fossadalsjökull*	1620	560	4.7	7
viii.	*Esjufjöll –Esjudalsjökull*	1700	500	16.0	33
ix.	*Esjufjöll –Esjujökull*	1640	940	2.1	1.5
x.	*Esjufjöll – Austurbjargajökull*	1500	560	15.1	11
xi.	*Esjufjöll – Flekksjökull*	1500	460	16.2	5.5
Norðlingalægðarjökull – Eastern arm					**499**
xii.	*Esjufjöll – Nyrðri Esjufjallajökull*	1700	10–20	38.5	109
xiii.	*Norðlingalægð – Breiðabunga*	1640	10–20	40.5	345
xiv.	*Eyjólfsfell – Snæfell*	1360	360	20.0	44
Þverártindsegg mountain					**28**
xv.	*Svöludalsjökull*	1540	680	5.6	12
xvi.	*Skrekkur (2 glaciers)*	1540	760	1.6	1.9
xvii.	*Fellsárjökull*	1500	560	5.3	9.6
xviii.	*Other small glaciers (total of 11)*	-	-	-	4.6
Overall area of Breiðamerkurjökull and Veðurárdalsjöklar in 2010					**934**

2.6.2 Area changes since LIA_{max}

Comparison of the three DEMs (1890, 1945 and 2010) shows great changes in the ice-covered area, the terminus and the bordering mountains, Breiðamerkurfjall and Veðurárdalsfjöll (Figure 24). From the DEMs 3D images were constructed in Surfer for visualisation of the development of the recession (Figure 25). A number of nunataks have been exposed in the ablation zone (Appendix B). In total, the glacier lost ~11% of its area, since the maximum extent in 1890. Table 8 summarizes the area changes for specified time intervals. The area loss of the Esjufjöll glaciers, from 75 km^2 to 58 km^2, is included. The area distribution with altitude is presented for each arm in Figure 26.

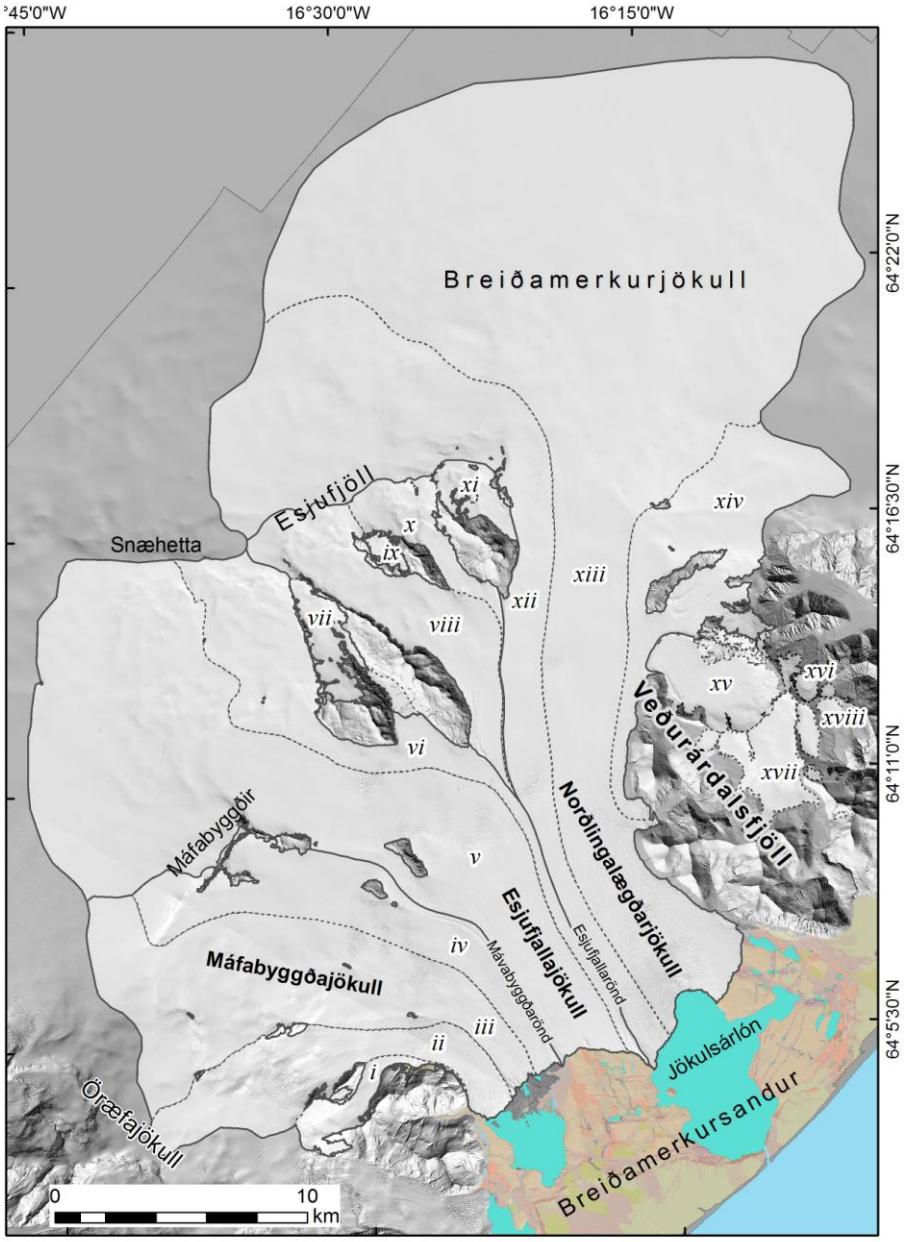

Figure 23. The three major arms of Breiðamerkurjökull divided into 14 individual glacier branches. Numbers refer to Table 7. Glaciers in Þverártindsegg mountain are included in table 7 and are also shown here.

Table 8. Recession of Breiðamerkurjökull since the LIA_{max}. First two columns (grey shaded) give the ice-covered area at the specific time and col. 3 gives the are of nunataks.

Year	Area (km^2)	Nunataks (km^2)	Period	Years	Area loss (km^2)	Area loss (%)	Area loss rate (km^2/yr)
1890	1020	17	1890–2010	120	114	11.2	0. 95
1945	987	21	1890–1945	55	33	3.2	0.60
2010	906	36	1945–2010	65	81	8.2	1.24

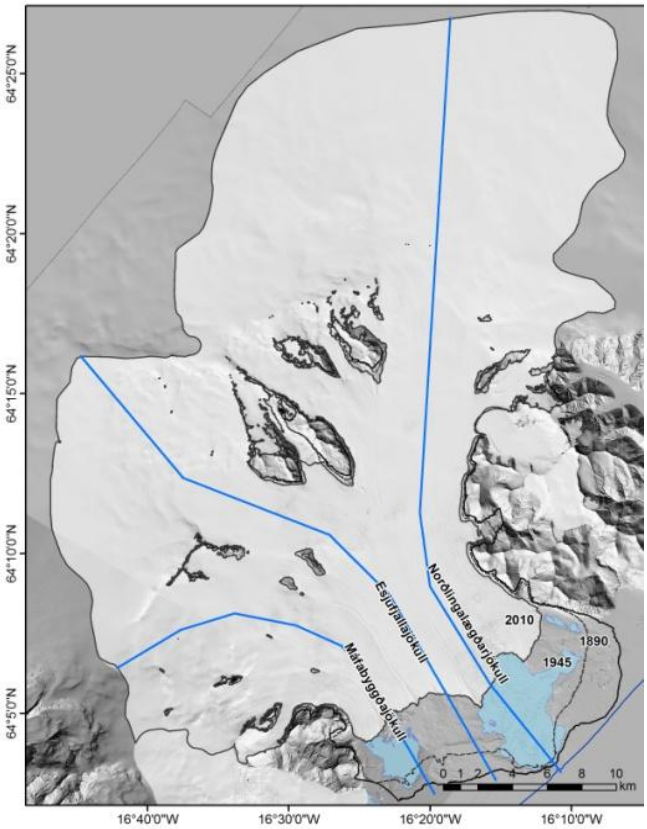

Figure 24. Area changes of Breiðamerkurjökull since LIA_{max} to the present (2010). Longitudinal profiles of the three arms are shown in Figure 25.

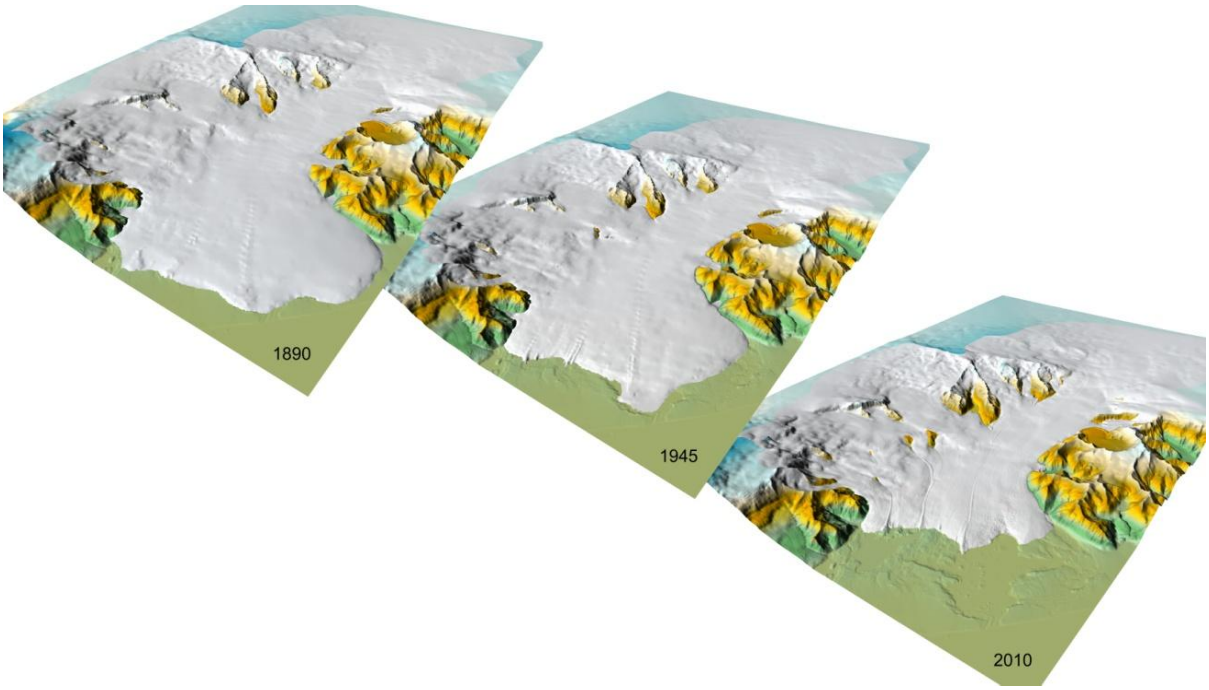

Figure 25. Perspective views of Breiðamerkurjökull in 1890, 1945 and 2010.

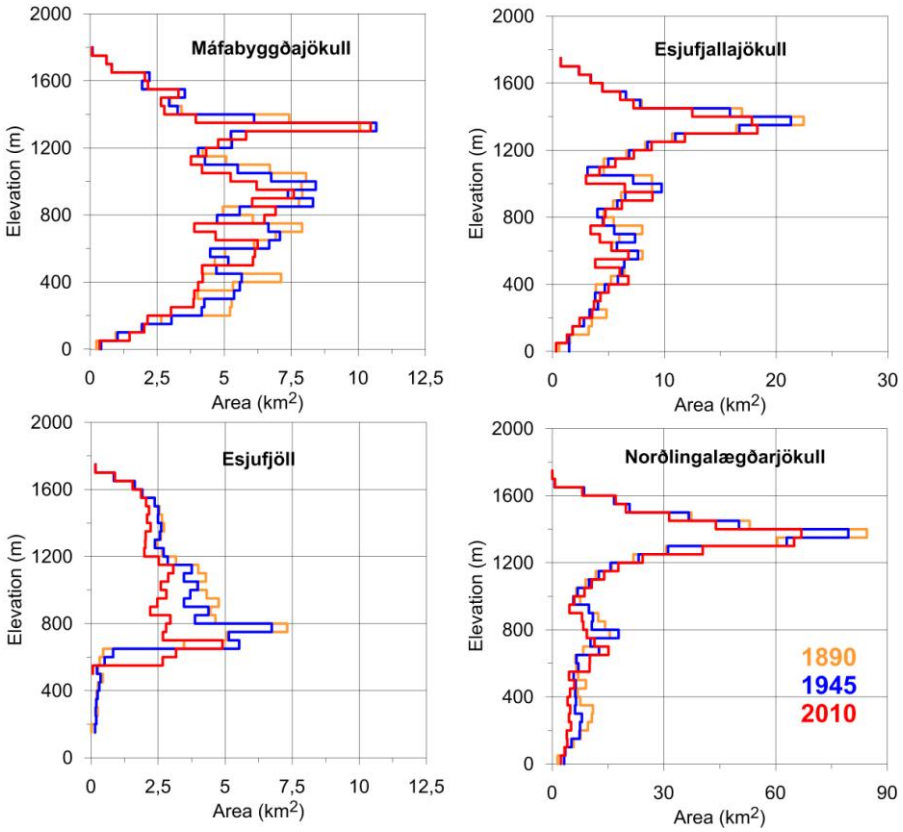

Figure 26. The area distribution (x-axis, note scale in km^2) of 1890, 1945 and 2010 with altitude (y-axis). At present the ELA is situated at about 1100–1200 m.

2.6.3 Longitudinal profiles since the LIA$_{max}$

At the end of the 19th century, the length of the terminus of Breiðamerkurjökull was 21 km, from Fellsfjall in the east to Fjallsjökull at the west. Adjoining Fjallsjökull and Hrútárjökull added other 7.5 km to the width of the terminus. The Norðlingalægðarjökull snout was 12.3 km wide, reaching to center of Esjufjallarönd. From there towards west the termini of Esjufjallajökull and Máfabyggðajökull were 4.7 km and 4 km long, respectively. The slope of the snout varied, ranging between 10° to 25°. Since then the outlet has retreated >5 km inland of which almost 2/3 has occurred after 1945.

Longitudinal profiles were drawn along the centre flowline of each arm from head to terminus. The profiles show a similar development for these branches, with maximum thickness reduction of >250 m at the location of 2010 terminus and little thickness change in the interior.

The retreat pace has been affected by variations in the climate. To estimate the variablility the terminus location was depicted at various times, from maps and photographs. The length from end-moraines to the snout was estimated at 15 different locations along the terminus, seven for Norðlingalægðarjökull, four and three for Esjufjalla- and Máfabyggðajökull, respectively. Measured lengths were then averaged for each arm. Table 9 represent the rate of the retreat of each arm. The periods depend on the years when the terminus was mapped. Note that the 1930 terminus has been traced for the Norðlingarlægðarjökull arm but not accurately for the others. The retreat rate is also presented graphically in Figure 28.

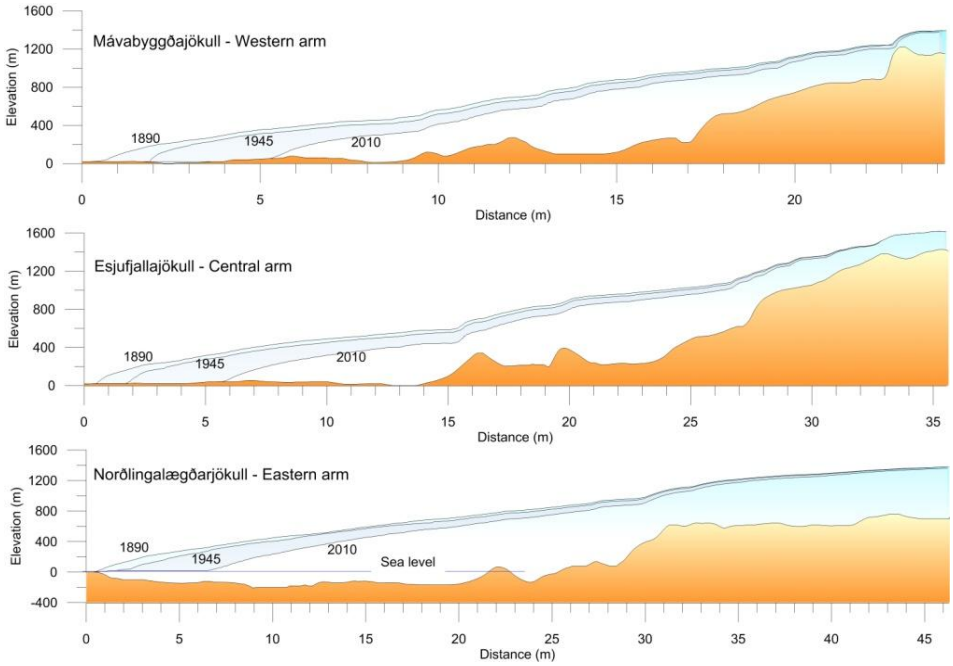

Figure 27. Longitudinal profiles of the three major arms of Breiðamerkurjökull based on the reconstructed DEMs and the LiDAR DEM. The bedrock was measured with by radio-echo sounding in 1991.

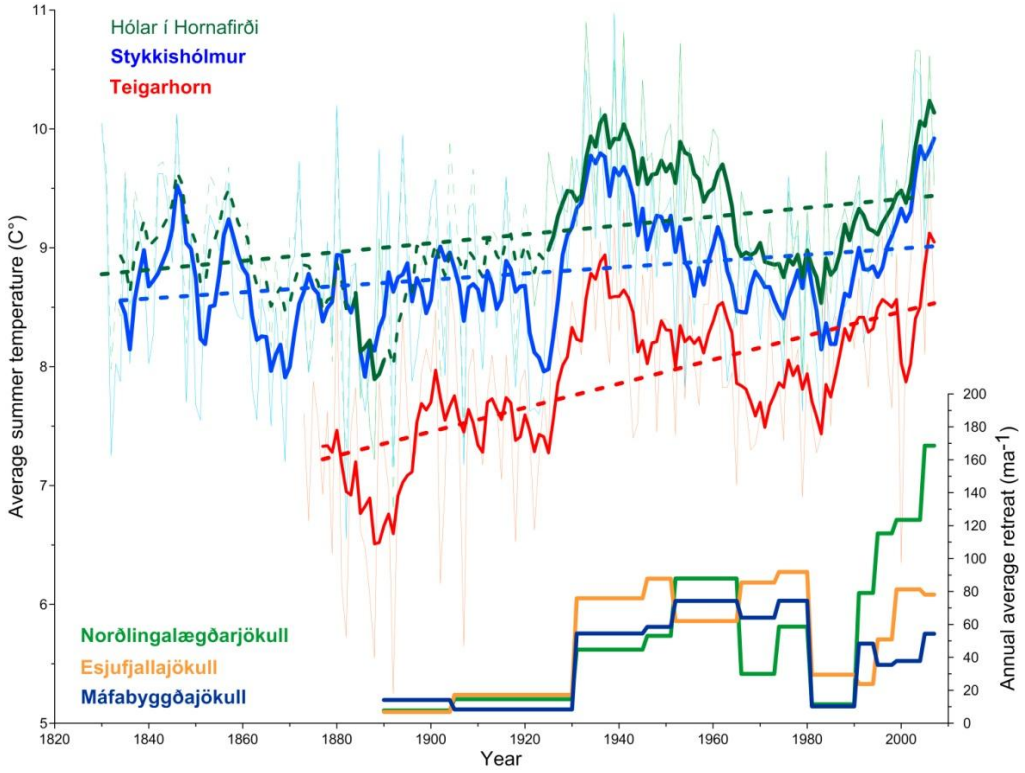

Figure 28. Variation of the termini of Breiðamerkurjökull together with the average summer temperature (above) during the late LIA to present (five years running average) from three weather stations; Stykkishólmur, West Iceland (since 1830), Teigarhorn (since 1873) and Hólar in East Iceland. The measurements at Hólar started in 1884, were discontinued in 1890 and were established again in 1921 (data from Icelandic Meteorological Office). The series (dotted line) was extended based on the Stykkishólmur data back to 1830 (Aðalgeirsdóttir et al., 2011). The lower part of the figure shows the annual average retreat (right vertical axis) of the terminus for each arm. The Norðlingarlægðarjökull outlet is calving into Jökulsárlón lagoon.

Table 9. Retreat rate of the main branches of Breiðamerkurjökull, between 1890 and 2010. The last row sums the total retreat from LIA_{max} to 2010.

Period	Norðlingalægðarjökull		Esjufjallajökull		Máfabyggðajökull	
	Retreat (m)	ma^{-1}	Retreat (m)	ma^{-1}	Retreat (m)	ma^{-1}
1890–1904	109	8	198	7	134	14
1904–1930	365	15	–	–	–	–
1930–1945	626	45	–	–	–	–
1904–1945	–	–	1493	37	972	24
1945–1951	265	53	439	88	293	59
1951–1965	1143	88	807	62	966	74
1965–1973	210	30	598	85	449	64
1973–1980	352	59	551	92	446	74
1980–1990	104	12	266	30	92	10
1990–1994	237	79	72	24	145	48
1994–1998	346	115	153	51	106	35
1998–2004	618	124	406	81	189	38
2004–2010	843	169	391	78	272	54
1890–2010	5216	66	5270	58	4127	45

2.6.4 Volume changes since the LIA_{max}

Estimates of volume changes were calculated by subtracting DEMs. The 2010 surface was subtracted from the LIA_{max} DEM and the 1945 surface DEM. Moreover, the subglacial DEM was subtracted from all three ice surface DEMs to calculate the total ice volume of the glacier. The volume is calculated assuming that the trench below sea level was excavated during the LIA and fully developed at the end of 19th century.

Table 10 shows the derived volume changes and Figure 29 the same results graphically. Volume differences between two surfaces is given for the whole period or separately for the periods 1890–1945 and 1945–2010. The volume is given both as ice and water equivalent.

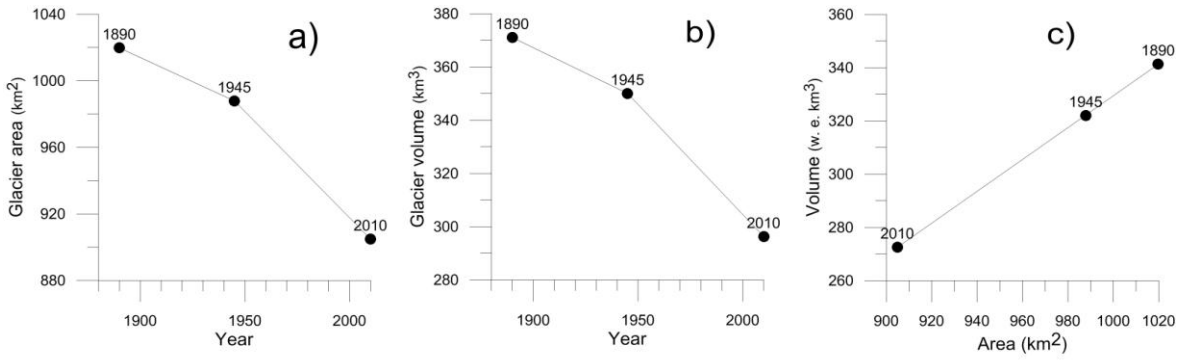

Figure 29. Changes of Breiðamerkurjökull from 1890 to 2010. a) area and b) ice volume. Both show increased rate of change after 1945, c) ice volume as a function of area.

Table 10. Volume changes since LIA_{max}. Period and numbers of years in first two columns, volume loss as ice and as into water equivalent (w. e.). Annual Average Volume Loss (AAVL) and annual average specific mass balance in w.e.. The total volume of the glacier is calculated assuming that the subglacial trench was fully evolved at the end of the LIA_{max}.

Period	Yrs	ΔV (ice km^3)	ΔV (w. e. km^3)	AAVL (km^3/yr)	ma^{-1}	Year	V (ice km^3)	V (w. e. km^3)
1890–2010	120	77.2	69.5 ± 8	0.58	-0.64	**1890**	371	341
1890–1945	55	21.0	18.9 ± 2	0.34	-0.17	**1945**	350	322
1945–2010	65	56.2	50.6 ± 6	0.78	-0.78	**2010**	299	275

**Estimated 11.5% error in volume.*

2.6.5 The ELA in 1890, 1945 and 2010

The accumulation/ablation area ratio in 1890 was estimated from the ELA in the late 19th century corresponding to zero balance values. This was also done for 1945 and the present day. The ELA varied between 1100–1200 m a.s.l., in 2002–2013 on Breiðamerkurjökull. A number of MODIS images captured in the autumn before the first winter snow were collected. Several were interpreted in ArcGIS to distinguish the border between snow and ice (Figure 30). These data were used side by side with the MODIS images and LiDAR DEM to estimate the ELA. The average ELA for these years was estimated as ~1140 m.a.s.l.. This estimate agrees with field measurements of mass balance on the Norðlingalægðarjökull arm (F. Pálsson, personal communication, 30 March 2014). The ELA was found at lower elevation (~900 m) on the eastern flanks of Öræfajökull than on Norðlingarlægðarjökull. This elevation was used to estimate the relative proportion of the accumulation area of Breiðamerkurjökull in 2010.

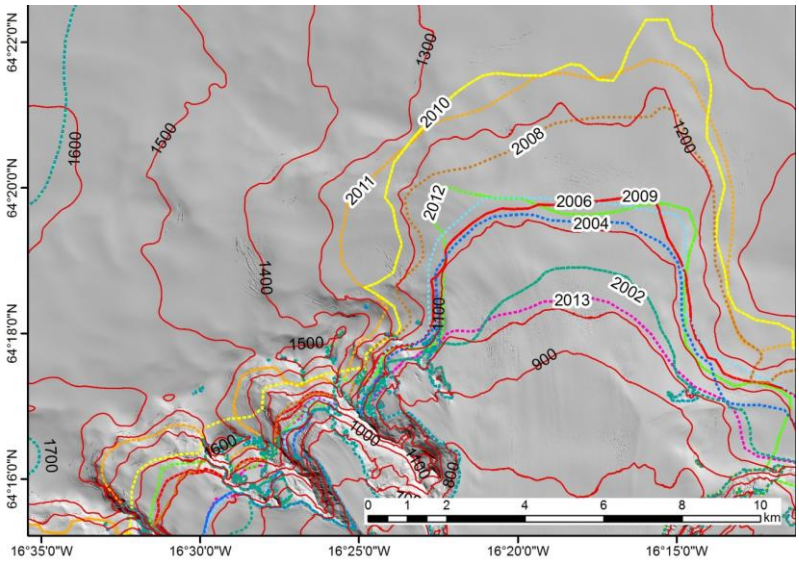

Figure 30. The ELA on Norðlingalægðarjökull arm and Esjufjöll, based on MODIS images in 2002–2013, varies widely in altitude. Averaging these results the ELA is at about 1150 m on this glacier arm but lower on the eastern flanks of Öræfajökull at ~900 m.

In the 1890s Thoroddsen (1931) reported the snowline ranging from elevation of 690 m in the eastern part of Öræfajökull to 880 m on the southern outlets of Vatnajökull, as far as the Mýrar district in Southeast Iceland, about 50 km distance to the east. An inclination of 3.8 m/km would position the snowline approximately 110 m higher in the Þverártindsegg mountain range than in Breiðamerkurfjall to the west and at average of 750 m on

Breiðamerkurjökull. Thoroddsen estimated that the snowline on southern Vatnajökull was 2400 feet (800 m). On the basis of these sparse observations we can speculate about the elevation of the 1890 ELA. Several authors have estimated that the ELA dropped to 750–700 m in Southern Iceland near the end of the LIA (Eyþórsson, 1951; Þórarinsson, 1974; Björnsson, 1998; Björnsson & Pálsson, 2008).

From the AMS aerial photographs we estimate the ELA of 1945, ranging on Breiðamerkurjökull from 1000 to above 1100 m. A difference of the ELA is observed across the wast outlet and even within the same outlet branch. The ELA on Öræfajökull is lower. Despite this variability we estimate the average 1945 ELA at 1100 m. Table 11 presents the estimated accumulation area ratio (AAR) of Breiðamerkurjökull in 1880, based on Thoroddsen (1931), our estimation for 1945 and the early 21st century average ELA (from MODIS).

Table 11. The ELA of Breiðamerkurjökull and the accumulation and ablation area ratio in the late 19th century, 1945 and 2010. The AAR ratio of the accumulation area to the total area of the basin.

Year	ELA average	Area			AAR
		Accumulation (km^2)	Ablation (km^2)	Total (km^2)	
1890s	~800	724	296	1020	0.71
1945	1100	548	439	987	0.56
2010	1140	486	420	906	0.53

2.7 Discussion

Digital elevation models of Breiðamerkurjökull at the 1890 LIA highstand and the year 1945, have been constructed and compared with an accurate LiDAR DEM from 2010. The LIA_{max} DEM was derived from geomorphological field evidence and DEMs produced from topographical maps by the DGS and AMS from 1904 and 1945, respectively after revision, elimination of errors and corrections.

Our DEMs allow quantitative estimates of the changes of Breiðamerkurjökull since the LIA and show that Breiðamerkurjökull has lost ~11% of its area and 20% of its volume since then. Of the total glacier area loss of 114 km^2 since LIA_{max} to 2010, about 29% occurred before 1945. About 19 km^2 of land and nunataks has been exposed within the present day (2010) ice margin. The greatest changes are found in the Esjufjöll range where mountain valley glaciers have lost more than 1/5 of their area since the end of the LIA exposing an area of more than 2 km^2 as nunataks, most of them below 1300 m elevation.

Annual average recession rate doubled in the later half of the 20th century. The retreat varied between the three main branches but was in general slow until 1930. Annual changes of the terminus then accelerated but a ten year interval of slower retreat started at around 1980. Since then the retreat of terminus has accelerated. The variation of the retreat rate with time is clearly related to the climate (Figure 28). The rapid retreat of Norðlingalægðarjökull, is caused by ice loss to Jökulsárlón lagoon by calving.

Earlier estimates of the recession of Breiðamerkurjökull, by Sigbjarnarson (1970) were based on data prior to 1970 which suffered from inaccurate elevation models of the interior regions of Vatnajökull. The area of the ice flow basin was overestimated by more than 150 km^2, as the

ice divides were depicted to far to the north. Sigbjarnarson estimated a thinning of about ~210 m at the terminus to no change above 1600 m elevation. This is in fair agreement with our results. The same appplies to his estimate of a mean annual area reduction, of 0.6 km^2/yr, from LIA_{max} (which he assumed to be in 1894) to 1945. He estimated an ice volume loss of 21.2 km^3 from 1894 to 1945, about 0.5 km^3/yr. Our results are an annual loss of 0.34 km^3/yr, in total of 21 km^3 reduction in ice volume, equivalent to 19.3 km^3 of water (Table 10).

During years of zero mass balance the accumulation area has typically been 55–65% of the total area on Icelandic glaciers (Björnsson & Pálssson, 2008; Björnsson, 2009). If the ELA on Breiðamerkurjökull had remained at below 800 m during LIA_{max} as suggested by Þórarinsson (1974), the accumulation area ratio (AAR) would have been 0.7 (Table 11). Such a high AAR would explain the advance of Breiðamerkurjökull during the LIA. During the advance the ablation zone expanded in area and we might expect that near the end of the 19th century the glacier had approached an equilibrium after centuries of advance. Near the end of the LIA the average ELA on Breiðamerkurjökull might have been somewhat higher (Thoroddsen, 1931).

The ELA has risen since the late 19th century to present and the AAR has consequently been reduced. From the 1945 aerial photographs we estimated an ELA at ~1100 m corresponding to an accumulation area ratio of 0.56. In 2010, the ratio had decreased to 0.53. This inevitably leads to continued retreat of Breiðamerkurjökull in the future as predicted by several authors (see e. g. Björnsson, Pálsson & Guðmundsson, 2001; Björnsson, 2009).

In the first decade of the 21st century the average AAR of the Esjufjöll mountain glaciers has been as low as 0.31. These small valley glaciers within the Esjufjöll region do not contribute much to the main Breiðamerkurjökull outlet as a whole. The larger arms, emanating from Snæhettudalur and Norðlingalægð, drag their snout into an elongated form. They disappear long before reaching the terminus. Esjudalsjökull (viii) however, reached down to the main terminus in 1890. If no large glaciers were situated on either site of these small glaciers they would only have formed small local snouts in front of the Esjufjöll mountain.

The area distribution with elevation is variable for the various arms of Breiðamerkurjökull (Figure 26) and changes in the ELA have different relative impact on the branches as a consequence. For an ELA of 1100 m about 70% of the total area of the easternmost branch, Norðlingalægðarjökull, would be an accumulation area, about 50% of Esjufjallajökull, 40% of Esjufjöll and close to 30% of Máfabyggðajökull. Even for an ELA of 1200 m, the AAR of Norðlingalægðarjökull would be close to 0.6. This easternmost arm is nevertheless retreating faster than any of the others. This indicates that the dynamic instabilty due to calving into the Jökulsárlón lagoon and the associated oscillation of ice flow towards the lagoon is the driving the downwasting of this arm (Björnsson, 1996). The retreat of the calving front in recent years indicates that rapid changes of the area distribution may be expected in the near future.

2.8 Conclusions

New LiDAR ice surface measurements make it possible to reconstruct old glacier surfaces by using data from existing topographical maps and photographs. Errors can be corrected based on deviations from the LiDAR map and DEMs of the ice surface at past times can be constructed.

The terminus of Breiðamerkurjökull has retreated >5 km on average since the late 19th century to 2010. The retreat varies along the terminus, ranging from 4 to 6 km on land but over 7 km where the glacier calves into Jökulsárlón lagoon.

In 2010, about 114 km^2 of previously ice-covered land (inside the former 1890 ice margin) had been exposed. From 1890 to 1945 the glacier area loss, due to the retreat of the terminus, was 33 km^2 or 0.95 km^2/yr. From 1945 to 2010 another 81 km^2 became ice-free were, i. e. up or 1.24 km^2/yr (see table 8).

About 19 km^2 of previously ice-covered land, has been exposed due to the thinning of the adjacent glacier in the Esjufjöll mountains. The ice-covered area was reduced from 75 km^2 to 58 km^2, i. e. by 22%.

The surface lowering of the Breiðamerkurjökull from LIA_{max} to 2010, represents a loss of 69.5 ± 8 km^3 w.e. This corresponds to 2003 20ft standard shipping containers (holding 33 m^3) every hour, from 1890 to 2010.

In 1890–1945 18.9 ± 2 km^3 w.e. was lost (0.34 km^3/yr) and 50.6 ± 6 km3 w.e. in the period 1945–2010 period (annual 0.78 km^3/yr). The last value would exhaust the total ice volume of Breiðamerkurjökull in 400 years.

Our LIA_{max} DEM, supported by the 1904 DGS map, implies that the prominent nunataks Kárasker and Bræðrasker were buried under >100 m thick ice at the end of the 19th century. It indicates that the glacier south of the peak of Máfabyggðir, Fingurbjörg, has thinned by ~85 m. It should be noted that this specified part of the glacier is mostly below the present day ELA.

A number of previously subglacial peaks became exposed in the 20th century and after 2000, mostly below an elevation of 1300 m (Appendix B). All such “skerrys” above 1300 m are clearly visible on the 1945 aerial photographs.

The ELA of Breiðamerkurjökull in the 1890s seems to have been somewhat higher than suggested by Thoroddsen (i. e. ~800 m, 2400 fet), and presumably it was between 850 m and 950 m. This was at the end of the LIA advance of the glacier and a slow reccession had started. Hence, we may assume that the outlet was close to zero mass balance.

Several cases of surge events or glacier advance in limited parts of the terminus without instability at other parts may be related to the fact that the glacier branches emanate from different accumulation basins of Vatnajökull.

The study demonstrates the value of old maps and photographs as well as geomorphological field evidence for scientific analysis of past glacier surfaces.

2.9 Summary

We have reconstructed digital elevation models (DEMs) of Breiðamerkurjökull, one of the largest outlet glaciers of the Vatnajökull ice cap, SE-Iceland, during its highstand of 1890 (LIA_{max}) and 1945. The aim was to constrain area and volume changes of that specified time period. The models were constructed by use of several sources: LiDAR DEM from 2010–2011, aerial and oblique aerial photographs, topographical maps from 1904 and 1945, written historical documents along with geomorphological in-field evidences. From resulting models we estimate the outlets retreat to >5 km inland since the LIA_{max} to 2010 and ~114 km^2 of land has become exposed. In terms of average annual loss of glaciated area of about 0.95 km^2/yr of area being exposed at average to the year 2010. The specified time was divided into two periods; 1890–1945 [55 yr] and 1945–2010 [65 yr] to constrain area and volume changes. About 2/3 of the ice loss has occurred after the mid 20^{th} century. The responses are in accordance with climate changes and ice mass loss accelerated as summer temperature rises. The total volume loss is 69.5 ± 8 km^3 water equivalency (w.e.). This correspond to an average specific mass loss of 0.64 m w.e./yr for the 120 year period, of 0.34 km^3 w.e./yr, from 1890 to 1945 and 0.74 km^3 w.e./yr from 1945 to 2010.

Appendix A: Comparison of the elevation of peaks and survey points outside the glacier

A comparison was made of the elevation of peaks and survey points outside the glacier surveyed by the Danish General Staff in 1904 with LiDAR DEM 2010 in order to assess the accuracy of the 1904 mapping. The elevation difference for the surveyed summits is assumed to indicate the errors to expect in the 1904 surveying of the ice surface. Nameless peaks are landmarked with P (for peak or survey point) followed by the DGS 1904 altitude. The results are listed in the following tables.

Table 12. Noted peaks on the west margin of Breiðamerkurjökull and Fjallsjökull outlet glaciers and nunataks of Öræfajökull. Coordinates in ISN93 (meters x and y) in second and third columns. Elevation depicted from LiDAR DEM 2010 and 1904 maps and in last column elevation difference in metres.

Summit/Peak (P)	x(m)	y(m)	Elevation 1904 (m)	Elevation 2010 (m)	Difference (m)
Miðaftanstindur	625308	395397	618	609	9
Rákartindur	624762	396408	774	777	3
Eyðnatindur	623681	396745	858	840	+18
P 1120	620099	397242	1128	1120	+8
P 984	622032	398053	984	960	+24
P 928	622716	399016	928	920	+8
Káratindur	619032	397799	1575	1545	+35
Heljargnípa	619498	398566	1399	1380	+19
P 702	621508	400075	702	700	+2
Þuríðartindur	615194	399773	1741	1730	+14
				StDev 11.4 – Average error	14

Table 13. Comparison of peaks and surveyed elevation points in Máfabyggðir observed on the 1904 map of the Danish General Staff. Coordinates in ISN93 (meters x and y) in second and third columns, and elevation depicted from LiDAR DEM 2010 and 1904 maps and in last column elevation difference.

Summit/Point (P)	x(m)	y(m)	Elevation 1904 (m)	Elevation 2010 (m)	Difference (m)
P 1432	615822	408054	1432	1415	+17
P 1449	615911	408076	1449	1430	+19
Kaplaklif	616570	407672	>1180	1190	+10
P 1114	617078	407753	1114	1110	+4
P 1327	616920	409821	1327	1320	+7
P 1194	617853	409367	1194	1180	+14
P 1327	616922	409814	1327	1325	+2
Fingurbjörg	618291	409307	1137	1130	+7
P 1019	619025	409233	1019	1000	+19
P 1094	617852	409368	1094	1080	+14
				StDev 6.5 – Average error	11

Table 14. Altitude of peaks in Vesturbjörg and Skálabjörg ridges, some surveyed by the Danish General Staff and shown on the 1904 map. Coordinates in ISN93 (meters x and y) in second and third columns, and elevation depicted from LiDAR DEM 2010 and 1904 maps and in last column elevation difference.

Summit/Peak (P)	x(m)	y(m)	Elevation 1904 (m)	Elevation 2010 (m)	Difference (m)
Vesturbjörg					
P 1500	618829	419180	1508	1500	+8
P 1465	618909	418936	1444	1465	21
P 1380	619356	417690	1384	1380	+4
P 1350	619420	417511	1331	1350	19
Snókur	619792	416371	1304	1304	0
P 1225	619894	415774	1234	1225	+9
P 1332	620119	415412	1335	1332	+3
P 1205	621503	414629	1203	1205	2
P 1185	620070	414371	1170	1185	15
				StDev 10,8 – Average error	3
Skálabjörg					
P 1470	619767	419142	1522	1470	+52
P 1300	621691	418087	1288	1300	12
P 1165	622751	417097	1103	1165	62
P 1055	623874	416652	1050	1055	+5
P 1205	623380	416296	1206	1205	+1
				StDev 40.6 – Average error	5

Table 15. Compared peaks and elevation points in Þverártindsegg mountains surveyed by the Danish General Staff in 1904. Coordinates in ISN93 (meters x and y) and elevation depicted from LiDAR DEM 2010 and 1904 maps and in last column elevation difference.

Summit/Peak (P)	x(m)	y(m)	Elevation 1904 (m)	Elevation 2010 (m)	Difference (m)
Eyjólfsfell	633262	418882	926	915	+11
Eyjólfsfell P 880	634131	419898	907	880	+27
Karl	637220	419476	1088	1075	+13
P 1130	637465	419744	1142	1130	+12
Snæfell	637146	417186	1383	1370	+13
P 1295	636475	417479	>1300	1295	>5
P 1221	636030	417595	1221	1210	+11
Þverártindsegg	638441	415130	1554	1540	+14
P 1415	639336	414661	1420	1415	+5
P 1195	638970	412641	1202	1195	+7
P 1160	639237	412302	1160	1160	0
P 1125	641004	410531	1132	1125	+7
Þverártindur	641181	410279	1113	1105	+8
Bæjartindur	643280	408386	848	850	2
				StDev 7.2 – Average error	9

Table 16. Compared peaks and elevation points in Veðurárdalsfjöll mountains surveyed by the Danish General Staff in 1904. Coordinates in ISN93 (meters x and y) and elevation depicted from LiDAR DEM 2010 and 1904 maps and in last column elevation difference.

Summit/Peak (P)	**x(m)**	**y(m)**	**Elevation 1904 (m)**	**Elevation 2010 (m)**	**Difference (m)**
P 1003	633367	414787	1003	1000	+3
P 1065	633855	414149	1076	1065	+11
P 1120	635020	413984	1124	1115	+4
P 1210	635853	413464	1222	1210	+12
Veðurárdalstindur	636220	413665	1240	1235	+5
P 1245	636909	413542	1252	1245	+7
Veðurárdalskambur	635661	412940	1203	1190	+13
P 1105	634957	412629	1114	1105	+9
P 1070	633190	413019	1076	1070	+6
Prestfell	633245	411743	1006	995	+11
Fauski	633825	408894	944	940	+4
Útigönguháls	634726	407825	823	820	+3
Hvítingsdalstindur	637983	409622	1112	1130	18
Miðfellstindur	637267	409107	1106	1125	20
Vestra Miðfell	637373	407385	946	945	+1
Fellsfjall	639486	405964	803	795	+8
				StDev 9.5 – Average error	4

Appendix B: Nunataks and rock outcrops exposed in the 20th century

A number of nunataks and rock outcrops were exposed in the 20th century and became more prominent in the 21st century. First these were depicted from LiDAR DEM and compared to aerial photographs from 1945 and 1982 to estimate area changes. Rock outcrops at high elevation showed no area changes implying little or no subsidence on the adjacent glacier surface. Lower in the accumulation area and towards the ablation zone, where geomorphological remnants are sparse, the surface lowering was traced on these nunataks and rocky outcrops, adding valuable information about the lowering of the glacier surface.

From a number of data points and construction of the average linear trend along the longitudinal axis following tables were compiled. In them all nunataks <1 km^2 (in 2010) are registered and thickness changes estimated.

Table 17. Prominent nunataks in Breiðamerkurjökull, south of Esjufjöll mountains and Máfabyggðir cliffs. Name/identification, coordinates in ISN93 (meters x and y) and elevation of the adjacent glacier surface in 1890, 1945 and 2010. Then thickness changes (surface lowering). Area in 1945 depicted from aerial photographs (Army Map Service, 1950) and 2010 (LiDAR DEM).

Nunatak	x(m)	y(m)	Elevation (m)			Thickness change (m)			Area (km^2)	
			1890	1945	2010	1890–1945	1945–2010	Total	1945	2010
Kárasker	622642	409005	860	820	750	40	70	110	0.10*[1]	0.98
Bræðrasker$_a$	621701	407368	840	810	750	30	60	90	–*[2]	0.39
Bræðrasker$_b$	622891	406640	700	675	560	25	105	130	–	0.02
Systrasker	623473	402185	630	580	490	50	90	140	–*[3]	0.07
Maríusker	620922	404236	800	770	690	30	80	110	–*[4]	0.02
S 825	619797	409042	910	890	825	20	65	85	–	0.01

**[1] Subglacial until mid 1930. *[2] Subglacial ~1960's. *[3] Subglacial until ~2000. *[4] Subglacial until ~2008.*

Table 18. Nunataks and rock outcrops in Snæhettudalur valley. Name/identification, coordinates in ISN93 (meters x and y) and elevation of the adjacent glacier surface in 1890, 1945 and 2010. Then thickness changes (surface lowering). Area in 1945 depicted from aerial photographs 1945 (Army Map Service, 1950) and 2010 (LiDAR DEM).

Nunatak	x(m)	y(m)	Elevation (m)			Thickness change (m)			Area (km^2)	
			1890	1945	2010	1890–1945	1945–2010	Total	1945	2010
S 1090	617695	414717	1150	1130	1090	20	40	60	–*5	0.004
S 1110	617752	414880	1160	1150	1110	10	40	50	–*5	0.004
S 1400	615400	417234	1400	1395	1380	5	15	20	–	0.004
S 1515	615013	418723	1515	1515	1500	–	15	15	–	0.004
S 1600	614605	419260	1600	1600	1600	–	–	0	–	–
Stakasker	608949	415482	1480	1480	1470	–	10	10	0.002	0.006
S 1045	619824	414789	1090	1080	1045	10	35	45	–	0.004

**5 Subglacial in 1989.*

Table 19. Nunataks and rock outcrops near Esjufjöll and the eastern part of the Snæhetta crest. Name/identification, coordinates in ISN93 (meters x and y) and elevation of lowest and highest part in 1890, 1945 and 2010. Area in 1945 depicted from AMS maps and aerial photographs (Army Map Service, 1950) and 2010 (LiDAR DEM).

Nunatak	**$x_{(m)}$**	**$y_{(m)}$**	**Elevation (m)**			**Thickness change (m)**			**Area (km^2)**	
			1890	**1945**	**2010**	**1890–1945**	**1945–2010**	**Total**	**1945**	**2010**
P 1220	619563	416849	1200	1190	1150	10	40	50	0.006	0.01
S 1145	619692	417028	1160	1150	1145	10	10	20	–	–
S 1595 a[1]	621078	422684	1590	1590	1590	–	–	–	0.006	–
S 1595 b[1]	621224	422755	1590	1590	1590	–	–	–	–	0.001
S 1495[2]	622950	423498	1495	1495	1490	–	5	5	0.0002	0.0005
S 1516[2]	623315	423547	1500	1500	1490	–	10	10	0.002	0.004
S 1540[2]	623648	423495	1520	1520	1520	–	–	–	0.002	0.001
S 1512 [2]	623733	423378	1500	1500	1500	–	–	–	0.0003	0.001
P 1502[3]	623819	423295	1500	1500	1500	–	–	–	–	–
Uggi N	624477	423822	1520	1520	1520	–	–	–	–	–
Uggi S	624564	423523	1420	1420	~1410	–	10	10	–	–
H 1525	624784	424183	1480	1480	~1470	–	10	10	0.009	0.015
S 1382[4]	625419	424883	1380	1375	1365	5	10	15	0.001	0.002
S 1326	625942	424144	1320	1310	1290	10	20	30	0.025	0.035
S 1226	626726	424472	1260	1250	1220	10	30	40	–	0.003
S 1152[5]	627171	424925	1200	1185	1140	15	45	60	–	0.011
S 1110[6]	627230	424288	1160	1140	1100	20	40	60	–	0.011
S 1074[7]	627262	424058	1130	1110	1060	20	50	80	–	0.003
S 1136[8]	627057	424033	1170	1160	1120	10	40	50	0.004	0.019
S 1122[9]	626913	423938	1170	1150	1120	20	30	50	–	–
S 1088[10]	626935	423759	1120	1110	1180	10	30	40	–	0.003
S 1090[11]	626919	423638	1090	1060	1015	30	45	75	0.0016	0.317
S 1005[11]	627240	423036	1000	980	920	20	60	80	0.0015	*1
S 1104[12]	625961	423145	1100	1085	1030	15	55	70	0.004	0.158
S 1035[12]	626156	422904	1070	1040	1000	30	40	70	0.006	*2
S 1276[13]	625254	423063	1300	1285	1260	15	25	40	0.001	0.015
S 1180[14]	625350	422759	1180	1170	1120	10	50	60	0.006	0.027
S 1152[14]	625394	422666	1155	1145	1100	10	45	55	0.0002	*3
S 1097[15]	625543	422643	1145	1125	1070	20	55	75	–	–
S 1022[16]	633718	422823	1080	1060	1020	20	40	60	–	0.13
S 900	633980	420835	960	940	880	20	60	80	–	0.01

[1] Two equally high rocks in H 1595. [2] Four rocks in western slopes of H 1545. [3] Rocky ridge south of H 1545. [4] Rockspire 0,95 km northeast from H 1525. [5]Furthest to east of reckognized rocks on Esjufjöll's high crest. [6] Largest one of a four small rocks. [7] Small rock south of S 1110. [8] Rock west of S 1074. [9] About 177 m southwest of S 1136 but belongs to that rock. [10] South of S 1122. [11] S 1090 og S 1005 separated in 1945 but now belonging to the same rock outcrop (2010). [12] S 1104 og S 1035 now belonging to the same rock outcrop (2010). [13] About 720 m west of S 1035. [14] S 1180 og S 1152 now belonging to the same rock outcrop (2010). [15] S 1097 is southeast of S 1180. [16] S 1022 is 3,5 km north from Eyjólfsfell mountain.

**[1] Same rock as above. *[2] Same rock as above. *[3] Same rock as above.*

References

Introduction

Aðalgeirsdóttir, G., S. Guðmundsson, H. Björnsson, F. Pálsson, T. Jóhannesson, H. Hannesdóttir, S. Þ. Sigurðsson & E. Berthier 2011. Modelling the 20th and 21st century evolution of Hoffellsjökull glacier, SE-Vatnajökull, Iceland. *The Cryosphere*, 5, 961–975, 2011. doi:10.5194/tc-5-961-2011. Website: sciencedirect.com.

Auriac, A., K. H. Spaans, F. Sigmundsson, A. Hooper, P. Schmidt & B. Lund 2013. Iceland rising: Solid Earth response to ice retreat inferred from satellite radar interferometry and visocelastic modeling, *J. Geophys. Res*., 118, doi:10.1029/2012JB009593.

Axford, Y., Á. Geirsdóttir, G. H. Miller & P. G. Langdon 2009. Climate of the Little Ice Age and the past 2000 years in northeast Iceland inferred from chironomids and other lake sediment proxies. *J Paleolimnol*, 41:7–24. doi 10.1007/s10933-008-9251-1. Website: sciencedirect.com.

Árnadóttir, T., B. Lund, W. Jiang, H. Geirsson, H. Björnsson, P. Einarsson & T. Sigurdsson 2009. Glacial rebound and plate spreading: results from the first countrywide GPS observations in Iceland. *Geophys. J. Int*. 177, 691–716.

Björnsson, H. 1996. Scales and rates of glacial sediment removal: a 20 km long, 300 m deep trench created beneath Breiðamerkurjökull during the Litle Ice Age. *Annals of Glaciology* 22, 141–146.

Björnsson, H. 2009. *Jöklar á Íslandi*. Bókaútgáfan Opna, Reykjavík, 479 pp.

Björnsson, H. & F. Pálsson 2008. Icelandic glaciers. *Jökull*, 58, 365–386.

Björnsson, H., F. Pálsson, S. Guðmundsson, E. Magnússon, G. Aðalgeirsdóttir, T. Jóhannesson, E. Berthier, O. Sigurðsson, and T. Thorsteinsson 2013. Contribution of Icelandic ice caps to sea level rise: Trends and variability since the Little Ice Age, Geophys. Res. Lett., 40, doi:10.1002/grl.50278.

Jóhannesson, T. & O. Sigurðsson 1998. Interpretation of glacier variations in Iceland 1930–1995. *Jökull*, 45, 27–33.

Jóhannesson, T., G. Aðalgeirsdóttir, H. Björnsson, P. Crochet, E. B. Elíasson, H. Ólafsson, F. Pálsson, Ó. Rögnvaldsson, O. Sigurðsson, Á Snorrason, Ó. G. Blöndal Sveinsson & Þ. Þorsteinsson 2007. *Effect of climate change on hydrology and hydro-resources in Iceland*. National Energy Authority – Hydrological Service, Reykjavík, 91 pp.

Magnússon, E., H. Björnsson, J. Dall & F. Pálsson 2005. The 20th century retreat of ice caps in Iceland derived from airborne SAR: W-Vatnajökull and N-Mýrdalsjökull. *Earth and Planetary Science Letters*, 237 (2005) 508–515. Website: sciencedirect.com.

Ogilvie, A. E. J., & Trausti Jónsson 2000. 'Little Ice Age' Research: A Perspective from Iceland. *Climatic Change* 48, 9–52.

Pagli, C., F. Sigmundsson, B. Lund, E. Sturkell, H. Geirsson, P. Einarsson, T. Árnadóttir, & S. Hreinsdóttir 2007. Glacio-isostatic deformation around the Vatnajökull ice cap, Iceland, induced by recent climate warming: GPS observations and finite element modeling. *Journal of Geophysical Research*, Vol. 112, doi: 10.1029/2006JB004421.

Pagli, C. & F. Sigmundsson 2008. Will present day glacier retreat increase volcanic activity? Stress induced by recent glacier retreat and its effect on magmatism at the Vatnajökull ice cap, Iceland. *Geophysical Research Letters*, 35, L09304, doi:10.1029/2008GL033510.

Sigmundsson, F., F. Albino, P. Schmidt, B. Lund, V. Pinel, A. Hooper & C. Pagli 2013. Multiple effects of ice load changes and associated stress change on magmatic systems. In *Climate Forcing of Geological Hazards, First Edition*. Edited by B. McGuire & M. Maslin. The Royal Society and John Wiley & Sons, Ltd.

Thoroddsen, Þ. 1931. *Lýsing Íslands*. 1.–2. bindi. Sjóður Þorvaldar Thoroddsen. Ísafoldar prentmiðja (reprinted 1931, 1. publication 1907–1911).

Watts, W. L. 1962. *Norður yfir Vatnajökul*. Icelandic transl. Jón Eyþórsson. Reykjavík. Bókfellsútgáfan, 1962. 208 pp.

Post-Little Ice Age volume loss of Kotárjökull glacier, SE-Iceland, derived from historical photography

Aðalgeirsdóttir, G., S. Guðmundsson, H. Björnsson, F. Pálsson, T. Jóhannesson, H. Hannesdóttir, S. Þ. Sigurðsson & E. Berthier 2011. Modelling the 20th and 21st century evolution of Hoffellsjökull glacier, SE-Vatnajökull, Iceland. *The Cryosphere*, 5, 961–975, 2011. doi:10.5194/tc-5-961-2011. Website: sciencedirect.com.

Björnsson, H. 1988. Hydrology of ice-caps in volcanic regions. *Soc. Sci. Isl.* 45, Reykjavík, 139 pp.

Björnsson, H., F. Pálsson, M. T. Guðmundsson & H. H. Haraldsson 1998. Mass balance of western and northern Vatnajökull, Iceland, 1991–1995. *Jökull*, 45, 35–58.

Björnsson, H. 2009. *Jöklar á Íslandi*. Bókaútgáfan Opna, Reykjavík, 479 pp.

Brown, M. E., C. Trujillo & D. Rabinowitz 2004. Discovery of a candidate inner Oort cloud planetoid. *Astrophysical J. Lett.* 10, 645–649.

Böðvarsson, Á. 1996. *Landmælingar og kortagerð Dana á Íslandi – Upphaf Landmælinga Íslands*. Landmælingar Íslands, Reykjavík. 316 pp.

Fagre, D. B., & L. A. McKeon 2010. Documenting Disappearing Glaciers: Repeat Photography at Glacier National Park, Montana. In: R. H. Webb, D. E. Boyer and R. M. Turner (eds.), *Repeat Photography: Methods and Applications in the Natural Sciences*, Island press, Washington D. C., 77–88.

Guðmundsson, M. T. 2000. Mass balance and precipitation on the summit of the plateau of Öræfajökull, SE Iceland. *Jökull,* 48, 49–54.

Guðmundsson, M. T. 2004. Vorferð Jöklarannsóknafélags Íslands, 4.–12. júní 2004. *Jökull,* 54, 135–138.

Guðmundsson, S. 1999. *Þar sem landið rís hæst, Öræfajökull og Öræfasveit*. Mál og menning, 183 pp.

Hannesdóttir, H., H. Björnsson, S. Guðmundsson, F. Pálsson, S. Guðmundsson, G. Aðalgeirsdóttir, S. Þ. Sigurðsson & H. Ágústsson 2012. 300 year history of glacier variations of SE Vatnajökull – a key to modelling their response to climate change. *Proc. 30th Nordic Geol. Winter Meeting*, Reykjavík, 55–56.

Harrison, A. E. 1960. *Exploring Glaciers with a Camera*. Sierra Club Books, San Francisco, CA, 71 pp.

Herforingjaráðið 1905. *Öræfajökull 87 SA.* Topographical map, 1:50.000. Kjöbenhavn, Geodætisk Inst. 1st ed.

Howell, F. W. W. 1892. The Öræfa Jökull, and its first ascent. *Proc. Royal Geographical Soc*. 14, 841–850.

Jóhannesson, T., H. Björnsson, E. Magnússon, S. Guðmundsson, F. Pálsson, O. Sigurðsson, T. Thorsteinsson & E. Berthier. 2013. Ice-volume changes, bias-estimation of mass-balance measurements and changes in subglacial water bodies derived by LiDAR-mapping of the surface of Icelandic glaciers. *Annals of Glaciology*, 54 (63), 63–74.

Koch, J. P. 1905–1906. Fra Generalstabens topografiske Avdelings Virksomhed paa Island. *Geografisk Tidsskrift,* 18, 1–14.

Luckman, B. H., TA . Kavanach, I. Craig & R. S. St. George 1999. Earliest photograph of Athabasca and Dome glaciers, Alberta. *Géographie physique et Quaternaire* 53(3), 401–405.

Magnússon, E., H. Björnsson, F. Pálsson & S. Guðmundsson 2012. The ice capped Öræfajökull volcano, SE-Iceland, surveyed with radio echo sounding. *Jökull*, 62, 131–150.

Molnia, B. F. 2010. Repeat photography of Alaskan Glaciers and Landscapes from Ground-Based Photo Stations and Airborne Platforms. In: R. H.Webb, D. E. Boyer & R. M. Turner (eds.), Repeat *Photography: Methods and Applications in the Natural Sciences*, Island press, Washington D.C, 59–76.

Morgunblaðið 2005. Hæðarbreyting á 100 ára fresti ætti engan að græta. Morgunblaðið 7. ágúst.

Ponzi F. 2004. *Ísland Howells – Howell's Iceland*. Brennholtsútgáfa, Mosfellsbær. 214 pp.

Thoroddsen, Þ. 1896. Ferð um Austur-Skaftafellssýslu og Múlasýslur sumarið 1894. *Andvari,* 21, 1–33.

Webb, R. H., R. M. Turner & D. E. Boyer 2010. Introduction: A brief history of repeat photography. In: R.H. Webb, D.E. Boyer, R.M. Turner (eds.), *Repeat Photography: Methods and Applications in the Natural Sciences*, Island Press, Washington D.C., 3–11.

Þórarinsson, S. 1943. Vatnajökull; Scientific results of the Swedish-Icelandic investigations 1936-37-38. Chapter 11. Oscillations of the Icelandic Glaciers in the last 250 years. *Geografiska Annaler*, 25 (1–2), 1–54.

Changes of the Breiðamerkurjökull outlet glacier, SE-Iceland, from its maximum extent in the late 19th century to the present

Aðalgeirsdóttir, G., S. Guðmundsson, H. Björnsson, F. Pálsson, T. Jóhannesson, H. Hannesdóttir, S. Þ. Sigurðsson & E. Berthier 2011. Modelling the 20th and 21st century evolution of Hoffellsjökull glacier, SE-Vatnajökull, Iceland. *The Cryosphere*, 5, 961–975, 2011. doi:10.5194/tc-5-961-2011. Website: sciencedirect.com.

AMS 1950. Army Map Service, Corps of Engineer; *6019 I Veðurárdalsfjöll, 6019 II Breiðamerkurjökull, 6019 III Öræfajökull, 6019 IV Esjufjöll, 6020 II Vatnajökull II and 6020 III Vatnajökull III. 1:50000*. Landmælingar Íslands. Website: www.lmi.is

Björnsson, F. 1998. Samtíningur um jökla milli Fells og Staðarfjalls. *Jökull*, 46, 49–61.

Björnsson, H. 1996. Scales and rates of glacial sediment removal: a 20 km long, 300 m deep trench created beneath Breiðamerkurjökull during the Litle Ice Age. *Annals of Glaciology*, 22, 141–146.

Björnsson, H., F. Pálsson & E. Magnússon 1999. *Breytingar á Jökulsárlóni 1934–1998*. Raunvísindastofnun Háskólans. Desember 1999. RH-29-99.

Björnsson, Helgi 1998. Frá Breiðumörk til jökulsands: mótun lands í þúsund ár. *Kvískerjabók*. Gísli Sverrir Árnason (editor). Höfn í Hornafirði, Sýslusafn Austur-Skaftafellssýslu.164–176.

Björnsson, H. 2009. *Jöklar á Íslandi*. Bókaútgáfan Opna, Reykjavík, 479 pp.

Björnsson, H., F. Pálsson & M. T. Guðmundsson 1992. *Breiðamerkurjökull. Niðurstöður íssjármælinga 1991*. University of Iceland. Science Institute. Reykjavík (RH-92-12).

Björnsson, H. & F. Pálsson 2008. Icelandic glaciers. *Jökull*, 58, 365–386.

Björnsson, H., F. Pálsson, O. Sigurðsson & G. E. Flowers 2003. Surges of glaciers in Iceland, *Annals of Glaciology*, 36, 82–90.

Björnsson, H., F. Pálsson, & S. Gudmundsson 2001. Jökulsárlón at Breidamerkursandur, Vatnajökull, Iceland: 20th century changes and future outlook. *Jökull*, 50, 1–18.

Björnsson, H., F. Pálsson, S. Guðmundsson, E. Magnússon, G. Aðalgeirsdóttir, T. Jóhannesson, E. Berthier, O. Sigurðsson, & T. Thorsteinsson 2013. Contribution of Icelandic ice caps to sea level rise: Trends and variability since the Little Ice Age, *Geophys. Res. Lett.*, 40, doi:10.1002/grl.50278.

Björnsson, S. 1994. Breiðamerkursandur. *Jökull*, 44, 57–59.

Boulton, G. S., K. Thors & J. Jarvis 1988. Dispersal of glacially derived sediment over part of the continental shelf of south Iceland and the geometry of the resultant sediment bodies. *Marine Geology*, 83, 1–4, 193–223.

Böðvarsson, Á. 1996. *Landmælingar og kortagerð Dana á Íslandi*. Landmælingar Íslands.

Dabski, M. & P. Angiel 2010. Geomorphic implications of the retreat of Breiðamerkurjökull in the southern part of the Skálabjörg ridge, Esjufjöll, Iceland. *Jökull,* 60, 185–198.

Durham University Iceland Expedition 1951. *Breiðamerkurjökull map 1951*. 1: 25000 scale map. Durham University.

Evans, D. J. A., & D. R. Twigg 2002. The active temperate glacial landsystem:a model based on Breidamerkurjokull and Fjallsjokull, Iceland. *Quaternary Science Reviews,* 21, 2143–2177.

Evans, D. J. A., & D. R. Twigg 2000. *Breiðamerkurjökull 1998.* 1:30000 scale map. University of Glasgow and Loughborough.

Eyþórsson, J. 1951. Þykkt Vatnajökuls. *Jökull,* 1, 1–6.

Eyþórsson, J. 1952 (a). Þættir úr sögu Breiðár. *Jökull,* 2, 17–20.

Eyþórsson, J. 1952 (b). Landið undir Vatnajökli. *Jökull,* 2, 1–4.

Frisak, H. 1812. *Hans Frisaks Dagboger for aaret 1812*. National and University Library of Iceland.

Guðmundsson, S., H. Hannesdóttir & H. Björnsson 2012. Post-Little Ice Age volume loss of Kotárjökull glacier, SE-Iceland, derived from historical photography. *Jökull,* 62, 97–110.

Guérin, C., Berthier, E., Björnsson, H., Guðmundsson, S., Magnússon, E. & Pálsson, F. 2010. *Velocity field, mass transport and calving of Breiðamerkurjökull, an outlet of Vatnajökull ice cap, Iceland, studied with satellite remote sensing and continuous GPS observations*. M.Sc. thesis.

Hannesdóttir, H., H. Björnsson, F. Pálsson, G. Aðalgeirsdóttir & Sv. Guðmundsson 2014. Volume and mass balance changes 1890–2010 of SE-Vatnajökull ice cap, Iceland. Ph.D. thesis submitted to the Cryosphere.

Henderson, E. 1957. *Iceland – or the Journal of a Residence in that island during the years 1814–1815*. Transl. Snæbjörn Jónsson; Ferðabók – frásagnir um ferðalög um þvert og endilangt Ísland árin 1814–1815, með vetursetu í Reykjavík. Prentsmiðja Hafnarfjarðar 1957. 456 pp.

Herforingjaráðið 1905. *Öræfajökull 87 SA, Öræfajökull – Esjufjöll 87 NA, Kálfafellstaður – Reynivellir 97 NV & Kálfafellstaður – Hrolllaugseyjar 97 NV. 1:50.000* (1st ed.). Generalstabens topografiske Afdeling. Geodætisk Inst., Kjöbenhavn. Landmælingar Íslands. Webpage: www.lmi.is/pages/vefthjonustur/kortasafn.

Howell, F. W. W. 1892. The Öræfa Jökull, and its first ascent. *Proc. Royal Geographical Soc*. 14, 841–850.

Howarth, P. J. & Welch, R. 1969(a). *Breiðamerkurjökull, August* 1965, *South East Iceland*. 1:30000. Department of Geography, University of Glasgow.

Howarth, P. J. & Welch, R. 1969(b). *Breiðamerkurjökull, August 1945*, *South East Iceland*. 1:30000. Department of Geography, University of Glasgow.

Jóhannesson, T., H. Björnsson, E. Magnússon, S. Guðmundsson, F. Pálsson, O. Sigurðsson, T. Thorsteinsson & E. Berthier 2013. Ice-volume changes, bias estimation of mass-balance measurements and changes in subglacial lakes derived by lidar mapping of the surface of Icelandic glaciers. *Annals of Glaciology*, 54, 63–74. doi 10.3189/2013aog63a422.

Jóhannesson, T., H. Björnsson, F. Pálsson, O. Sigurðsson & Þ. Þorsteinsson 2011. LiDAR mapping of the Snæfellsjökull ice cap, western Iceland. *Jökull,* 61, 19–32.

Jóhannesson, T. & O. Sigurðsson 1998. Interpretation of glacier variations in Iceland 1930-1995. *Jökull*, 45, 27–33.

Loftmyndir ehf© 2010. Aerial photographic database, Faculty of Earth Sciences, School of Engineering and Natural Sciences, University of Iceland.

Magnússon, Á. 1955. *Chorographica Islandica 1703*. Safn til sögu Íslands og íslenskra bókmennta. Hið íslenska bókmenntafélag 1955. Reykjavík.

MODIS 2013. Website: http://rapidfire.sci.gsfc.nasa.gov/

Pálsson, S. 1945. *Ferðabók Sveins Pálssonar. Dagbækur og ritgerðir 1791–1794*. Í Jón Eyþórsson, Pálmi Hannesson og Steindór Steindórsson (ritstj.og þýð.). 2. útgáfa. Reykjavík 1983. Örn og Örlygur.

Price, R. J. 1982. Changes in the proglacial area of Breiðamerkurjökull, southeastern Iceland: 1890–1980. *Jökull,* 32, 29–35.

Price, R.J., & Howarth, P. J. 1970. The evolution of the drainage system (1904–1965) in front of Breiðamerkurjökull, Iceland. *Jökull,* 20, 27–37.

Price, R. J. 1968. The University of Glasgow Breidamerkurjökull Project (1964–1967) – Progress report. *Jökull* 18, 389–394.

Rist, Sigurjón 1983. Jöklabreytingar 1964/65–1973/74 (10 ár), 1974/75–1980/81 (7 ár) og 1981/82. *Jökull,* 33, 141–144.

Sigbjarnarson, G. 1970. On the recession of Vatnajökull. *Jökull*, 20, 51–61.

Thoroddsen, Þ. 1959. *Ferðabók*, III. bindi. 2. útgáfa. Prentsmiðjan Oddi (1. útgáfa 1913–1915).

Thoroddsen, Þ. 1931. *Lýsing Íslands*. 1.–2. bindi. Sjóður Þorvaldar Thoroddsen. Ísafoldarprentsmiðja (endurprentun 1931, 1. útgáfa 1907–1911).

Tómasson, H. & E. Vilmundardóttir 1967. The lakes Stórisjór and Langisjór. *Jökull,* 17, 280–299.

Young, R. A. & D. E. StA. Harney 1951. *Esjufjöll July-September 1951*. Durham University Iceland Expedition.

Þórarinsson, S. 1956. *The thousand years struggle against ice and fire*. Two lectures delivered 21 and 26. february 1952 at Bedford College, London University. Bókaútgáfa Menningarsjóðs. Reykjavik 1956.

Þórarinsson, S. 1974. *Vötnin stríð – Saga Skeiðarárhlaupa og Grímsvatnagosa*. Bókaútgáfa Menningarsjóðs. Reykjavík.

Þórarinsson, S. 1943. Vatnajökull; Scientific results of the Swedish-Icelandic investigations 1936–37–38. Chapter 11. Oscillations of the Icelandic Glaciers in the last 250 years. *Geografiska Annaler* 25 (1–2), 1–54.

Watts, W. L. 1962. *Norður yfir Vatnajökul*. Icelandic transl. Jón Eyþórsson. Reykjavík. Bókfellsútgáfan, 1962. 208 pp.

bbprentun Höfn í Hornafirði